

## Review

# The advancements in mixed matrix membranes containing functionalized MOFs and 2D materials for CO<sub>2</sub>/N<sub>2</sub> separation and CO<sub>2</sub>/CH<sub>4</sub> separation



Guoqiang Li <sup>a,\*</sup>, Joanna Kujawa <sup>a</sup>, Katarzyna Knozowska <sup>a</sup>, Aivaras Kareiva <sup>b</sup>, Eric Favre <sup>c</sup>, Christophe Castel <sup>c</sup>, Wojciech Kujawski <sup>a,\*</sup>

<sup>a</sup> Faculty of Chemistry, Nicolaus Copernicus University in Toruń, Gagarina Street 7, Toruń 87-100, Poland

<sup>b</sup> Faculty of Chemistry and Geosciences, Vilnius University, Naugarduko str. 24, Vilnius LT-03225, Lithuania

<sup>c</sup> CNRS LRGP, Université de Lorraine, 1 Rue Grandville, Nancy F-54000, France

## ARTICLE INFO

## Key words:

CO<sub>2</sub> separation  
Mixed matrix membranes (MMMs)  
MOFs  
2D materials  
Filler functionalization

## ABSTRACT

CO<sub>2</sub> separation plays a crucial role in tackling the climate change induced by the greenhouse effects and improving the energy quality of natural gas and biogas. The efficient CO<sub>2</sub> separation technology is highly required. Membrane separation technology is particularly attractive in CO<sub>2</sub> separation processes owing to its advantages. However, the trade-off relationship limited the gas separation efficiency of polymeric membranes in gas separation processes. Therefore, it is necessary to prepare the high-performance membranes such as mixed matrix membranes (MMMs) for CO<sub>2</sub> separation. This review mainly focuses on the preparation methods, the material properties and the CO<sub>2</sub> separation efficiency of the MMMs containing various fillers such as modified ZIFs, MOFs, and GO, and the emerging MOF-based composites, 2D MOFs and 2D MXene. The modified fillers demonstrated higher compatibility with polymer matrix, resulting in enhanced mechanical stability and CO<sub>2</sub> separation efficiency of MMMs. 2D materials could significantly enhance the CO<sub>2</sub> separation efficiency of MMMs, owing to their layered structure and the effective regulation of gas transport ways. Finally, the future direction and conclusions of fillers and MMMs in gas separation processes are provided.

## 1. Introduction

The increase of global population, the fast development of the world economy, and the rapid industrialization process have led to a significant demand for energy (Jana & Modi, 2024). The majority of energy is from burning fossil fuels, which results in flue gas emissions into the

atmosphere (Jana & Modi, 2024). Flue gas mainly consists of N<sub>2</sub>, and CO<sub>2</sub>, along with a small amount of NO<sub>x</sub>, and SO<sub>x</sub>, etc., which is the largest source of CO<sub>2</sub> emissions (Dai & Deng, 2024). The greenhouse gas emissions, e.g., CO<sub>2</sub>, have caused climate change and global warming. In recent years, more and more extreme weather, wildfires, severe droughts, and floods have frequently appeared (Dai & Deng, 2024). The

**Abbreviations:** [Bmim][Tf<sub>2</sub>N], 1-butyl-3-methylimidazolium bis(trifluoromethanesulfonyl)imide; [MPPyr][DCA], Pyrrolidinium-based IL, 1-methyl-1-propyl pyrrolidinium dicyanamide; [P(3)HIm][Tf<sub>2</sub>N], 1-allyl-3H-imidazolium bis(trifluoromethanesulfonyl)imide; 2D, Two dimensional; A-prGO, Aminated partially reduced graphene oxide; APTMS, (3-Aminopropyl)trimethoxysilane; APTS, 3-Aminopropyltriethoxysilane; BDC, 1,4-benzenedicarboxylic acid; BET, Brunauer-Emmett-Teller; bPEI, Branched polyethyleneimine; BTC, Trimesic acid, Benzene-1,3,5-tricarboxylic acid; CA, Cellulose acetate; DLS, Dynamic light scattering; EDX, Energy-dispersive X-ray spectroscopy; FSM, Flat sheet membrane; FS-MMM, Flat sheet mixed matrix membrane; FTIR-ATR, Fourier Transform Infrared Spectroscopy with Attenuated Total Reflectance; GMA, Epoxy-containing glycidyl methacrylate; GO, Graphene oxide; HFM, Hollow fiber membrane; HF-MMM, Hollow fiber mixed matrix membrane; HKUST, Hong Kong University of Science and Technology; ICA, Imidazole-2-carbaldehyde; IL, Ionic liquid; MCNs, Microporous carbon nanoplates; MIL, Materials of Institute Lavoisier; MMM, Mixed matrix membrane; MOF, Metal organic framework; MUF, Massey University Framework; MWCNT, Multi-wall carbon nanotubes; NM, Maleic anhydride; PA, Polyamide; PDMS, Poly(dimethylsiloxane); Pebax, Poly(ether block amide); PEEK, Poly(ether ether ketone); PEG, Poly(ethylene glycol); PEGDE, Poly(ethylene glycol) diglycidyl ether; PEI, Polyetherimide; PES, polyethersulfone; PGO, Poly(glycidyl methacrylate-co-poly(oxyethylene methacrylate)); PHNZ, Polystyrene-acrylate (PSA) modified hollow NH<sub>2</sub>-ZIF-8 nanospheres; PI, Polyimide; PIL, Polymerized ionic liquid; PIM, Polymers of intrinsic microporosity; POEM, Poly(oxyethylene methacrylate); POSS, Polyhedral oligomeric silsesquioxane; PP, Polypropylene; PPO, Poly(p-phenylene oxide); PSf, Polysulfone; PSS, Poly(4-styrene sulfonate); PTMSP, Poly(1-trimethylsilyl-1-propyne); PTO, Poly(tetrahydrofurfuryl methacrylate)-co-poly(poly(oxyethylene methacrylate)); PU, Polyurethane; PVA, Poly(vinyl alcohol); PVAc, Polyvinyl acetate; PVAm, Polyvinylamine; PVDF, Polyvinylidene fluoride; PVP, Polyvinylpyrrolidone; RTIL, Room temperature ionic liquids; SEM, Scanning electron microscope; STEM, Scanning transmission electron microscopy; TFC-HFM, Thin film composite hollow fiber membrane; TFN, Thin film nanocomposite; TGA, Thermogravimetric analysis; UiO, University of Oslo; XRD, X-ray diffraction; ZIF, Zeolitic imidazolate framework.

\* Corresponding authors.

E-mail addresses: [grantli@umk.pl](mailto:grantli@umk.pl) (G. Li), [wkujawski@umk.pl](mailto:wkujawski@umk.pl) (W. Kujawski).

reduction of CO<sub>2</sub> emissions is important to tackle the environmental problems related to global warming (Zhang et al., 2022). The separation of CO<sub>2</sub> from flue gas is crucial for reducing CO<sub>2</sub> emissions.

Besides the separation of CO<sub>2</sub> from flue gas, the separation of CO<sub>2</sub> from natural gas and biogas is another industrial CO<sub>2</sub> separation application. Natural gas mainly contains methane and some other gas impurities (e.g., CO<sub>2</sub>, and H<sub>2</sub>S). The presence of gas impurities undermines the energy quality of natural gas and creates pipeline corrosion in the transporting process, which is problematic for its practical applications. Therefore, the gas impurities must be removed to purify the natural gas (Biondo et al., 2018; George et al., 2016). Biogas contains 50–70 vol% CH<sub>4</sub> and 30–50 vol% CO<sub>2</sub>, which is crucial for obtaining renewable energy since the limited fossil fuels are under depletion. However, to improve the energy quality and prevent the transporting pipelines' corrosion, CO<sub>2</sub> must be removed to purify biogas (Gong et al., 2020).

Chemical absorption (Ji et al., 2021), adsorption (Abd et al., 2021), and cryogenic separation (Yousef et al., 2018) are widely used technologies for CO<sub>2</sub> separation. However, these separation processes are either energy-consuming or unfriendly to the environment. Therefore, more efficient CO<sub>2</sub> capture technology is highly needed. Membrane separation technology is developed for CO<sub>2</sub> separation process. Comparing to the conventional technologies for CO<sub>2</sub> separation, e.g., chemical absorption and cryogenic process, membrane-based technologies for CO<sub>2</sub> separation have shown many advantages, such as lower capital and processing cost, high compactness and light weight, easy upscaling, low maintenance, lower energy consumption, and environmental friendliness (Xu et al., 2018; Li et al., 2015; Li et al., 2021). Therefore, membrane technology shows great potential and practical merit in the industrial CO<sub>2</sub> separation processes (Pasichnyk et al., 2023).

In the CO<sub>2</sub> separation processes, the gas transport properties of polymeric membranes was restricted by the Robeson upper bound (Fig. 1) (Robeson, 2008). The gas permeability and selectivity of polymeric membranes cannot be increased simultaneously. In order to break the trade-off relationship, the fabrication of mixed matrix membranes (MMMs) is considered as a desirable method since it can combine the merits of polymers and nanofillers (Al-Rowaili et al., 2023). However, to prepare defect-free MMMs, some issues must be considered and tackled. For example, filler agglomeration and poor dispersion might occur in the fabrication process of MMMs, which creates non-selective voids in MMMs. The particle size, the filler content, the interfacial interaction between fillers and polymer matrix, the dispersion of fillers in solvents,

and the polymer chain rigidification must be considered when preparing MMMs since they can influence the gas transport properties of MMMs (Kamble et al., 2021). Therefore, the functionalization of fillers is crucial to strengthen the compatibility between fillers and polymer matrix and simultaneously increase gas permeance and selectivity.

In this work, the CO<sub>2</sub> capture properties of MMMs containing modified ZIFs and MOFs, MOF-based composites, and emerging 2D materials, such as the functionalized GO, g-C<sub>3</sub>N<sub>4</sub>, 2D MOF nanosheets, and 2D MXene nanosheets will be comprehensively summarized and discussed. The modification methods for ZIFs, MOFs, and GO will be presented. The effects of modified ZIFs, MOFs, and GO on the membrane material properties and the CO<sub>2</sub> separation performance of MMMs will be discussed. In addition, the synthesis of emerging MOF-based composites and 2D fillers, e.g., 2D MOF nanosheets and 2D MXene nanosheets, and their effects on the membrane characteristics and gas permeability and selectivity of MMMs will be discussed. Finally, the perspectives and conclusions of CO<sub>2</sub> separation using MMMs are presented.

## 2. MMMs containing ZIFs and MOFs

ZIFs and MOFs are porous crystals consisting of metal nodes and organic ligands (Kujawa et al., 2021). ZIFs and MOFs possess uniform pore sizes, various topologies, high surface areas, small aperture size, high CO<sub>2</sub> affinity, connected channels for the transport of molecules, adjustable chemical and physical properties, and tailored functionalities, which makes ZIFs and MOFs suitable for various separation processes, especially for CO<sub>2</sub> separation using membranes (Zhu et al., 2021). For example, ZIF-8 possesses a small aperture equal to 3.4 Å, which is bigger than the kinetic diameter of CO<sub>2</sub> (3.3 Å) but smaller than the kinetic diameter of N<sub>2</sub> (3.6 Å) and CH<sub>4</sub> (3.8 Å) (Li et al., 2022). The porous structure of ZIF-8 can provide additional pathways for CO<sub>2</sub> molecules while inhibiting the transport of larger gas molecules, which allows the selective transport of CO<sub>2</sub> molecules through MMMs (Li et al., 2022). Moreover, ZIFs and MOFs showed higher CO<sub>2</sub> affinity and CO<sub>2</sub> adsorption capacity, which can further enhance the solubility of CO<sub>2</sub> molecules in MMMs (Mahajan & Lahtinen, 2022). Compared with other types of inorganic fillers, ZIFs, and MOFs have shown better compatibility and interaction with polymer matrix owing to their organic ligands, which is crucial for the preparation of defect-free MMMs (Kamble et al., 2021; Ozcan et al., 2024). The structures of some ZIFs and MOFs used in the preparation of MMMs are shown in Fig. 2 (Al-Rowaili et al., 2023). In

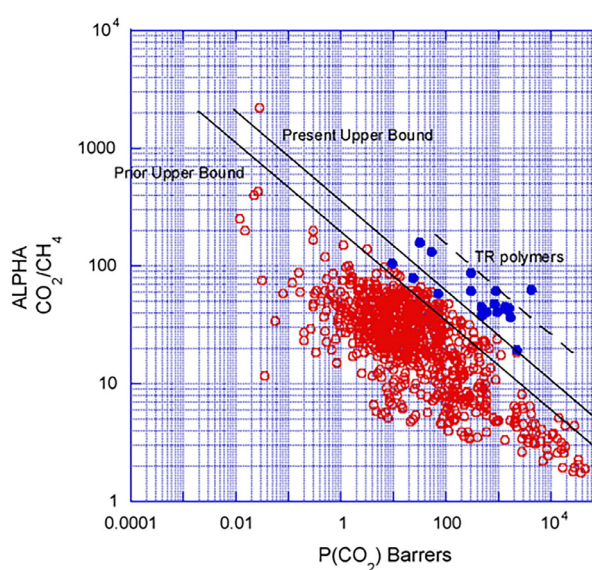
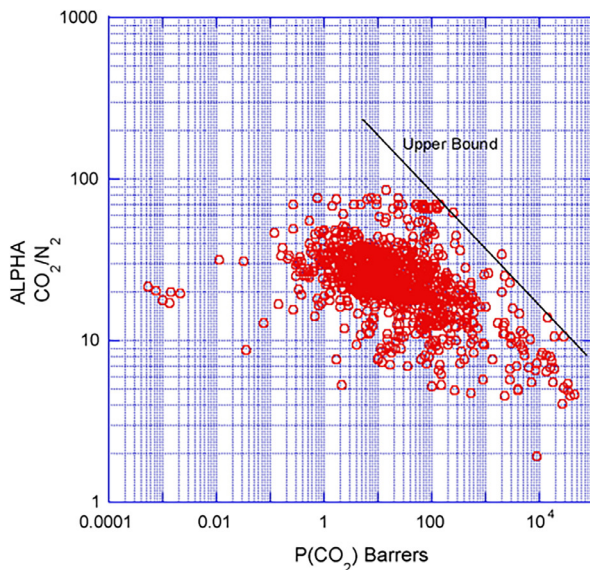


**Fig. 1.** The Robeson upper bound correlation for CO<sub>2</sub>/N<sub>2</sub> separation and CO<sub>2</sub>/CH<sub>4</sub> separation (Robeson, 2008). Reprinted with permission from Elsevier. Copyright 2008.

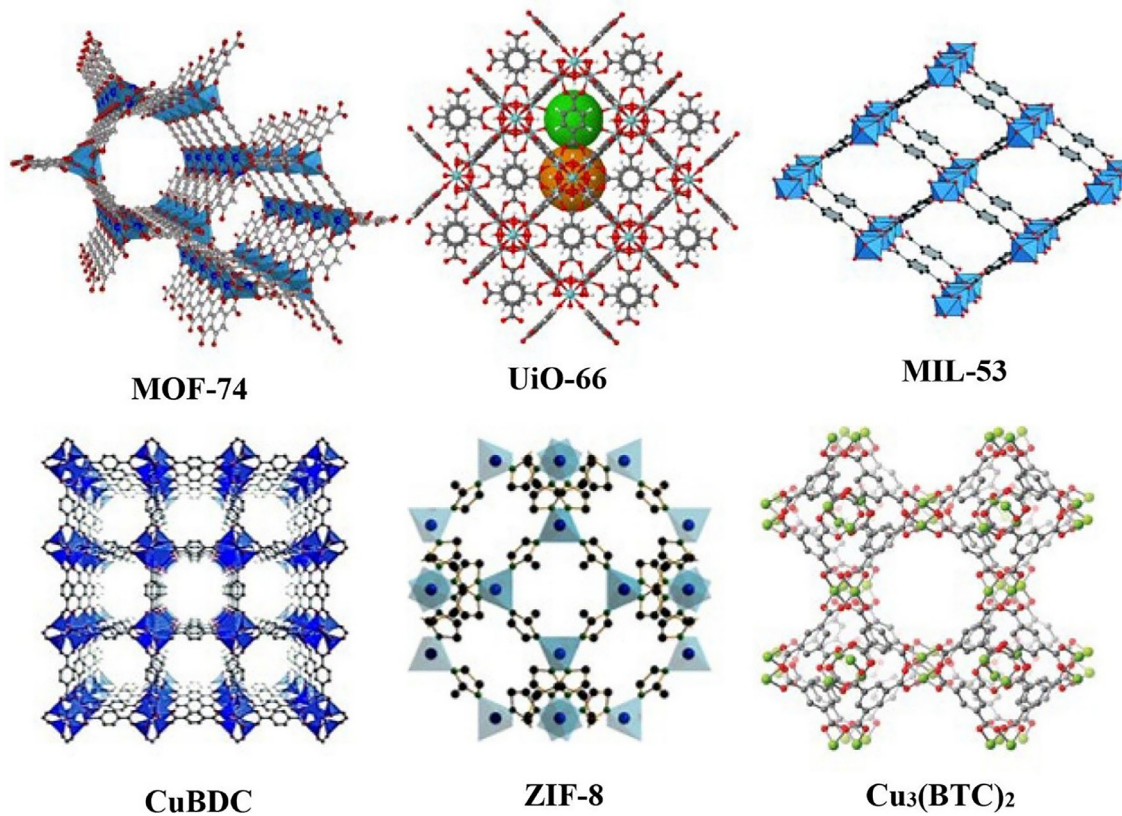


**Fig. 2.** The structure of some ZIFs and MOFs used in MMMs (Al-Rowaili et al., 2023). Reprinted with permission from Elsevier. Copyright 2023.

the preparation of MMMs for gas separation, the pore size and surface functionality of ZIFs and MOFs can be tuned *via* physical and chemical modification, endowing ZIFs and MOFs with precise molecular size sieving effect and high adsorption affinity for the target gas molecules (Kamble et al., 2021; Zhu et al., 2021). As a result, the modification of ZIFs and MOFs could further enhance the separation efficiency of gas molecules of MMMs. The modification of MOFs can be realized by two ways which are the post-synthetic modification (PSM), e.g., functionalization with amine group, functionalization with COOH group, functionalization using amino acid, ILs modified MOFs, and impregnation, and *in situ* modification e.g. the utilization of dual organic linkers or metal centers (Zhu et al., 2021). A PSM strategy can be conducted to modify metal clusters and organic ligands of MOFs and ZIFs, which enables the control of the cavity micro-environment and the crystal structure. Moreover, the PSM strategy can be used to prepare new MOFs and ZIFs which are difficult to synthesize *via* direct nucleation-growth method owing to the high energy barrier (Zhu et al., 2021; Li et al., 2022). In the *in situ* modification process, ions, molecules, or polymers were introduced into MOFs and ZIFs during the crystallization process. As a result, the *in situ* modification is more homogeneous, and the functionalities are well distributed with MOFs and ZIFs (Zhu et al., 2021). Therefore, the effects of various pristine and modified ZIFs and MOFs on the membrane properties and separation efficiency of gas molecules of MMMs are discussed in section 2.

### 2.1. MMMs containing ZIFs

ZIFs are caged crystalline compounds consisting of tetrahedrally coordinated metal center, i.e., Zn or Co divalent cations and imidazolate linkers. ZIFs have various structures, high specific surface area, tunable pore channels, small pore size (less than 0.5 nm), and the feasibility of easy functionalization (Imtiaz et al., 2022). Therefore, ZIFs have been

intensively investigated in MMMs for gas separation since they are able to enhance the separation efficiency of gas molecules of membranes.

Wang et al. (2021) synthesized ZIF-301 and incorporated it into the 6FDA-DAM polyimide matrix to fabricate ZIF-301/6FDA-DAM MMMs for CO<sub>2</sub>/CH<sub>4</sub> separation. The synthesized ZIF-301 possessed a Langmuir BET surface equal to 623.5 m<sup>2</sup>/g and a higher adsorption capacity for CO<sub>2</sub> (25.31 cm<sup>3</sup>/g) over CH<sub>4</sub> (9.30 cm<sup>3</sup>/g). ZIF-301 was homogeneously dispersed in a polyimide matrix without agglomeration with filler content up to 20 wt%. The MMMs containing 20 wt% of ZIF-301 showed the highest CO<sub>2</sub> permeability, equal to 891 Barrer, and CO<sub>2</sub>/CH<sub>4</sub> selectivity equal to 29.3, which is attributed to the high CO<sub>2</sub> affinity and the molecular sieving effect of ZIFs.

In an effort to improve ZIFs' compatibility with polymer matrix, the *in situ* modification strategy can be applied to modify ZIFs. Wang et al. (2020) synthesized nanoporous NH<sub>2</sub>-ZIF-7 by partially replacing benzimidazole with 2-aminobenzimidazole in ZIF-7. The synthesized NH<sub>2</sub>-ZIF-7 nanoparticles were incorporated into PIM-1 to prepare MMMs for biogas upgrading. It was found that NH<sub>2</sub>-ZIF-7 possesses a bigger window size than ZIF-7, which is beneficial for CO<sub>2</sub> transport. Moreover, NH<sub>2</sub>-ZIF-7 showed a high specific surface area and the ability of forming hydrogen bonds with polymer chains, which is helpful to inhibit the formation of defects in MMMs. As a result, the mechanical properties and the aging resistance of MMMs were improved. In comparison to the pristine PIM membranes, 20 wt% NH<sub>2</sub>-ZIF-7/PIM-1 MMMs demonstrated CO<sub>2</sub> permeability of 2953 Barrer and 65 % higher CO<sub>2</sub>/CH<sub>4</sub> selectivity of 21. The improvement of gas transport properties can be attributed to the intrinsic properties of NH<sub>2</sub>-ZIF-7, resulting in the increased diffusion selectivity of MMMs.

Besides the *in situ* modification, the post-synthetic modification (PSM) strategy was used to modify ZIF-8 by Li et al. (2022). ZIF-8 was firstly functionalized by branched polyethyleneimine (bPEI) and then modified with an ionic liquid (IL) (Fig. 3). Subsequently, ZIF-8@IL/Pebax MMMs were fabricated. It was discovered that ZIF-8's crys-

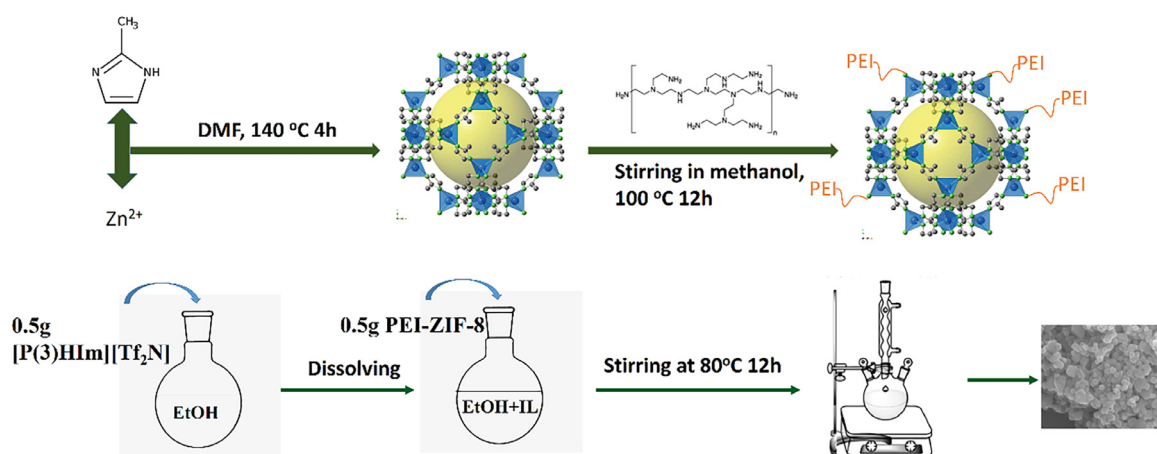


**Fig. 3.** The synthesis of ZIF-8, ZIF-8-PEI, and ZIF-8-PEI@[P(3)HIm][Tf<sub>2</sub>N] (Li et al., 2022). Reprinted with permission from Elsevier. Copyright 2022.

**Table 1**

Summary of separation efficiency of CO<sub>2</sub> molecules of MMMs containing ZIFs (SG - single gas, MG - mixed gas).

Polymers	MOFs	MOF content [wt%]	MOF content [wt%]	Gas pairs	P <sub>CO<sub>2</sub></sub> [Barer]	Selectivity	Testing conditions	Refs.
Matrimid®	ZIF-68	20	20	CO <sub>2</sub> /N <sub>2</sub>	27	30	35 °C, 10 bar, MG	van Essen et al. (2021)
				CO <sub>2</sub> /CH <sub>4</sub>	25	35		
6FDA-DAM	ZIF-301	20		CO <sub>2</sub> /CH <sub>4</sub>	891	29	25 °C, 4 bar, SG	Wang et al. (2021)
Polyimide (6FBDA)	ZIF-8-NH <sub>2</sub>	50	50	CO <sub>2</sub> /CH <sub>4</sub>	81	89	35 °C, 4.5 bar, SG	Zhao et al. (2024)
				CO <sub>2</sub> /N <sub>2</sub>	81	81		
P84	ZIF-8	27		CO <sub>2</sub> /CH <sub>4</sub>	11	93	25 °C, 3 bar, MG	Guo et al. (2018)
PES	Etched ZIF-8	10		CO <sub>2</sub> /N <sub>2</sub>	16	7	25 °C, 1 bar, SG	Zhou et al. (2020)
PIM-1	NH <sub>2</sub> -ZIF-7	20		CO <sub>2</sub> /CH <sub>4</sub>	2953	21	30 °C, 2 bar, SG	Wang et al. (2020)
	ZIF-7				2662	18		
PIM-1	ZIF-67	15		CO <sub>2</sub> /CH <sub>4</sub>	2800	21	30 °C, 2 bar, SG	Ye et al. (2020)
PIM-1	TSILs@ZIF-67	10		CO <sub>2</sub> /CH <sub>4</sub>	12848	11	23 °C, 1 bar, SG	Han et al. (2021)
PSf	ZIF-11	24		CO <sub>2</sub> /CH <sub>4</sub>	23	43	25 °C, 3 bar, MG	Guo et al. (2020)
PSf	ZIF-8	0.5		CO <sub>2</sub> /CH <sub>4</sub>	16 GPU	36	25 °C, 4 bar, SG	Kamaludin et al. (2023)
PSf	ZIF-78	10		CO <sub>2</sub> /N <sub>2</sub>	13	54	30 °C, SG	Wu & Chang, 2024
PSf	ZIF-8	5		CO <sub>2</sub> /CH <sub>4</sub>	420	19	30 °C, 6 bar, MG	Ban et al. (2015)
				CO <sub>2</sub> /N <sub>2</sub>	464	30		
	[bmim][Tf <sub>2</sub> N]@ZIF-8			CO <sub>2</sub> /CH <sub>4</sub>	312	38		
				CO <sub>2</sub> /N <sub>2</sub>	351	116		
Pebax 1657	[bmim][Tf <sub>2</sub> N]@ZIF-8	15		CO <sub>2</sub> /N <sub>2</sub>	105	84	25 °C, 1 bar, SG	Li et al. (2016)
				CO <sub>2</sub> /CH <sub>4</sub>	105	35		
	ZIF-8			CO <sub>2</sub> /N <sub>2</sub>	78	40		
				CO <sub>2</sub> /CH <sub>4</sub>	78	20		
Pebax 1657	NH <sub>2</sub> -ZIF-8	10		CO <sub>2</sub> /N <sub>2</sub>	115	60	25 °C, SG	Ding et al. (2022)
	PHNZ-2				122	97		
Pebax 1657	ZIF-8	7		CO <sub>2</sub> /CH <sub>4</sub>	450	32	25 °C, 2 bar, MG	Liang et al. (2023)
	PSS-ZIF-8				528	36		
Pebax 2533	ZIF-8	10		CO <sub>2</sub> /N <sub>2</sub>	266	34	25 °C, 2 bar, SG	Zhang et al. (2018)
	Zn/Ni-ZIF-8				321	43		
Pebax 2533	ZIF-8-	15		CO <sub>2</sub> /N <sub>2</sub>	285	76	24 °C, 2 bar, SG	Li et al. (2022)
	PEI@P(3)HIm][Tf <sub>2</sub> N]			CO <sub>2</sub> /CH <sub>4</sub>	25			
Pebax 2533	ZIF-67	16		CO <sub>2</sub> /N <sub>2</sub>	191	40	25 °C, 4 bar, SG	Maleh & Raisi, 2023
				CO <sub>2</sub> /CH <sub>4</sub>	23			
Pebax 1657	ZIF-8	5		CO <sub>2</sub> /N <sub>2</sub>	80	57	25 °C, 2 bar, SG	Wang et al. (2021)
	ZnO@ZIF-8 hollow nanotubes				140	67	25 °C, 5 bar, MG	
Maltitol modified	ZIF-8	5		CO <sub>2</sub> /N <sub>2</sub>	400	69	30 °C, 10 bar, SG	Nobakht & Abedini, 2023
Pebax 1657				CO <sub>2</sub> /CH <sub>4</sub>	2			
6FDA-Durene	ZIF-67	20		CO <sub>2</sub> /CH <sub>4</sub>	1250	25	35 °C, MG	Chen et al. (2021)
	Veiled ZIF-67	30			1210	33		

tal structure was entirely conserved upon modification. What is also essential, ZIF-8@IL was homogeneously dispersed in the polymer matrix owing to the formation of hydrogen bonds between amino groups and Pebax chains. As a result, the gas separation efficiency was dramatically enhanced in the fabricated MMMs. The size-sieving effects of ZIF-8@IL, the facilitated transport channels for CO<sub>2</sub>, and the increased CO<sub>2</sub> affinity to fillers contributed to the improvements in CO<sub>2</sub> separation efficiency.

As it is shown in Table 1, ZIF-7, ZIF-8, and ZIF-67 are the most studied ZIFs in the preparation of MMMs for CO<sub>2</sub> separation. Pebax, PIM-1, polysulfone, and polyimide are the commonly used polymers in the fabrication of MMMs containing ZIFs. The optimal filler content is between 5 and 50 wt%. It can be found the MMMs containing modified ZIFs showed higher CO<sub>2</sub> separation efficiency than MMMs containing pristine ZIFs.

## 2.2. MMMs containing UiO MOFs

UiO-66 is a type of MOF developed by the University of Oslo (Zou & Liu, 2019). The  $\text{Zr}_6\text{O}_4(\text{OH})_4$  nodes contain six  $\text{Zr}^{4+}$  ions in an octahedral geometry coordinated with four hydroxyl atoms (Rego et al., 2022). UiO-66 MOFs have high hydrothermal stability, high chemical stability, high surface area and tunable pore size, making them promising in preparing MMMs for gas separation. Furthermore, UiO-66-NH<sub>2</sub>, a derivative of UiO-66, exhibits a high capacity for CO<sub>2</sub> adsorption because of the base-acid and dipole-quadrupole interactions that occur between amino groups and CO<sub>2</sub> molecules (Jiang et al., 2019). Owing to the presence of an active -NH<sub>2</sub> group, UiO-66-NH<sub>2</sub> can be easily modified with other functional groups.

Thür et al. (2019) synthesized UiO-67 by partially substituting the biphenyl-4,4'-dicarboxylic acid (bpdc) linker with 2,2'-bipyridine-5,5'-dicarboxylic acid (bpydc) linker. The prepared UiO-67 nanoparticles were incorporated into a polyimide matrix to prepare MMMs for CO<sub>2</sub>/CH<sub>4</sub> separation. The synthesized UiO-67 containing 33 % bpydc showed 100 % higher CO<sub>2</sub>/CH<sub>4</sub> selectivity and 63 % higher CO<sub>2</sub> permeability, comparing with the pristine polyimide membranes. This is because the UiO-67-33 showed higher CO<sub>2</sub> affinity resulting from the Lewis acid-base interaction between the N sites in bpydc and CO<sub>2</sub> molecules. MMMs containing UiO-67-33 nanoparticles demonstrated a facilitated transport mechanism for CO<sub>2</sub> permeation. MMMs with 10 wt% of UiO-67-33 nanoparticles exhibited CO<sub>2</sub> permeability of 26 Barrer and CO<sub>2</sub>/CH<sub>4</sub> selectivity of 75.

Liu et al. (2020) modified UiO-66 with branched polyethyleneimine (PEI) and ionic liquid [bmim][Tf<sub>2</sub>N] to improve the CO<sub>2</sub>/CH<sub>4</sub> separation efficiency and the interfacial morphology of MMMs. The fabricated MMMs with 15 wt% UiO-66-PEI@[bmim][Tf<sub>2</sub>N] showed 100 % higher CO<sub>2</sub> permeability of 26 Barrer and 71 % higher CO<sub>2</sub>/CH<sub>4</sub> selectivity of 60, comparing with the pristine Matrimid membranes, comparing with the pristine membranes. This is because the presence of amino groups and the formation of hydrogen bonds improved the compatibility between MOF fillers and polymer matrix. The IL could provide CO<sub>2</sub> adsorption, which enhanced the CO<sub>2</sub> affinity of MMMs. The amino groups promoted the CO<sub>2</sub> permeation via the reversible reaction.

Lu et al. (2021) modified UiO-66-NH<sub>2</sub> with [bmim][Tf<sub>2</sub>N] ionic liquid (IL) by using the solvent immersion method. Subsequently, the UiO-66-NH<sub>2</sub>@IL was incorporated into PIM-1 matrix to prepare MMMs for CO<sub>2</sub>/N<sub>2</sub> separation (Fig. 4). The IL can act as a regulator between polymer and fillers, significantly improving their compatibility. The UiO-66-NH<sub>2</sub>@IL was homogeneously dispersed in PIM-1 matrix. The fabricated UiO-66-NH<sub>2</sub>@IL/PIM-1 MMMs exhibited high CO<sub>2</sub> permeability of 8283 Barrer and CO<sub>2</sub>/N<sub>2</sub> selectivity of 23. The additional pathways for CO<sub>2</sub> from the microporous UiO-66-NH<sub>2</sub> and the high affinity of IL and amino groups from UiO-66-NH<sub>2</sub>@IL contributed to the high efficiency of gas separation.

As it is shown in Table 2, UiO-66 and UiO-66-NH<sub>2</sub> are often used as fillers in MMMs for CO<sub>2</sub> separation. Pebax, PIM-1, and polyimide are the commonly used polymers in the fabrication of MMMs containing UiO. The filler content is between 10 wt% and 30 wt%. MMMs containing modified UiO showed higher CO<sub>2</sub> capture properties than MMMs containing unmodified UiO.

## 2.3. MMMs containing MIL MOFs

MIL is a type of MOF firstly reported by the Materials Institute Lavoisier (Loiseau et al., 2004). For example, the MIL-53 consists of trivalent metal cations such as In<sup>3+</sup>, Cr<sup>3+</sup>, Ga<sup>3+</sup>, Al<sup>3+</sup>, and Fe<sup>3+</sup> and the coordinated linear dicarboxylate linkers such as NH<sub>2</sub>-BDC and BDC (Schneemann et al., 2014). MILs have exhibited outstanding properties, e.g., high hydrothermal and chemical stability, high flexibility, tunable geometry, and pore size. These properties are desirable for the utilization of MIL MOFs in membrane separation, especially in gas separation by using MMMs (Al-Rowaili et al., 2023).

Habib et al. (2023) synthesized [MPPyr][DCA]/MIL-101(Cr) composite by using the wet impregnation method. Subsequently, the synthesized composite was utilized to fabricate Pebax-based MMMs for CO<sub>2</sub> separation. [MPPyr][DCA] ionic liquid was used as a modifier because it has high CO<sub>2</sub> solubility and less toxicity in comparison to imidazolium-based ionic liquids. It was found that the crystal structure of MIL-101(Cr) did not change after the modification with ionic liquid. The surface morphology of MIL-101(Cr) was barely affected (Fig. 5). However, the sur-

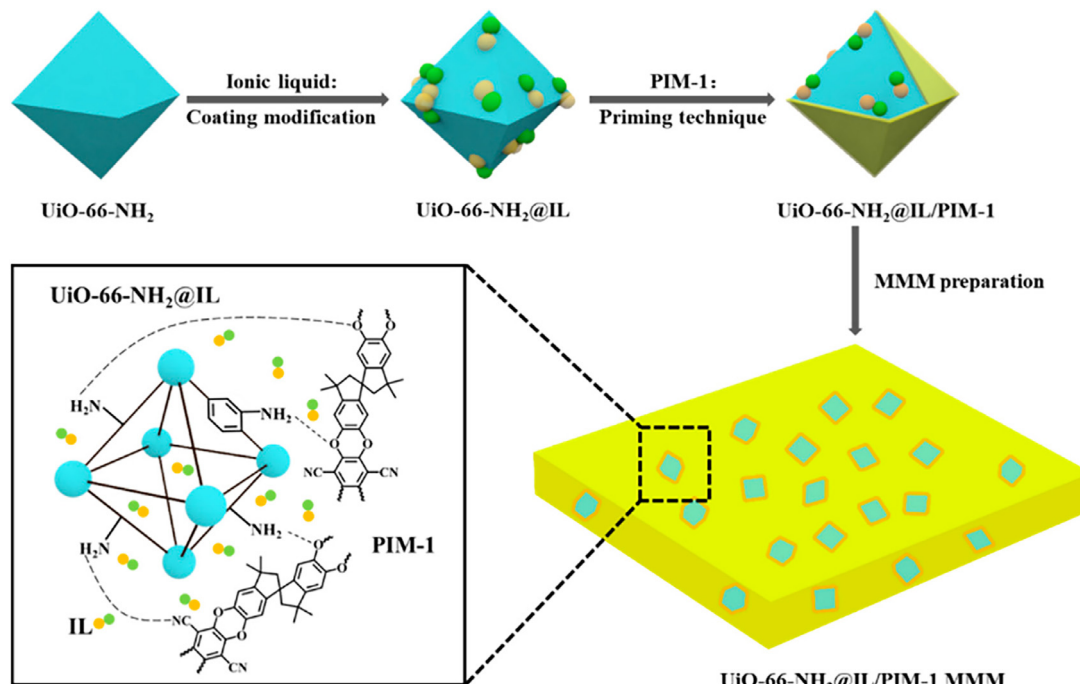


Fig. 4. The preparation process of UiO-66-NH<sub>2</sub>@IL/PIM-1 MMM (Lu et al., 2021). Copyright 2021 MDPI. CC BY 4.0 License.

**Table 2**Summary of separation efficiency of CO<sub>2</sub> molecules of MMMs containing UiO MOFs (SG - single gas, MG - mixed gas).

Polymers	MOFs	MOF content [wt%]	Gas pairs	P <sub>CO<sub>2</sub></sub> [Barrer]	Selectivity	Testing conditions	Refs.
Matrimid®	UiO-66-NH <sub>2</sub>	10	CO <sub>2</sub> /CH <sub>4</sub>	52	45	25 °C, 3 bar, MG	Jiang et al. (2019)
	UiO-66-NH <sub>2</sub> @ICA			40	65		
6FDA-ODA ODPA-TMPDA	UiO-66-PEI@[bmim][Tf <sub>2</sub> N]	15	CO <sub>2</sub> /CH <sub>4</sub>	26	60	35 °C, 1 bar, MG	Liu et al. (2020)
	UiO-66	20	CO <sub>2</sub> /N <sub>2</sub>	169	32	35 °C, 1 bar, MG	Chuah et al. (2020)
6FDA-DAM	UiO-66-NH <sub>2</sub>			142	37		
	UiO-66-Br			200	35		
	UiO-66-(OH) <sub>2</sub>			125	39		
	UiO-66	14	CO <sub>2</sub> /CH <sub>4</sub>	1912	31	35 °C, 2 bar, MG	Ahmad et al. (2018)
	UiO-66-NH <sub>2</sub>	16	CO <sub>2</sub> /CH <sub>4</sub>	1223	30		
PIM-1 PVA+PVAm/PS	UiO-66-NH-COCH <sub>3</sub>	16	CO <sub>2</sub> /CH <sub>4</sub>	1263	33		
	[bmim][Tf <sub>2</sub> N]@UiO-66-NH <sub>2</sub>	10	CO <sub>2</sub> /N <sub>2</sub>	8283	23	20 °C, 1 bar, SG	Lu et al. (2021)
	PEGDE-UiO-66-NH <sub>2</sub>	28.5	CO <sub>2</sub> /N <sub>2</sub>	1295 GPU	91	25 °C, 3 bar, MG	Xu et al. (2019)
PEI	UiO-66-NH <sub>2</sub> -PVP	18	CO <sub>2</sub> /H <sub>2</sub>	394	13	25 °C, MG	Ashtiani et al. (2021)
	UiO-66	10	CO <sub>2</sub> /CH <sub>4</sub>	400	33	25 °C, 1 bar, SG	Cui et al. (2024)
Pebax Polyurethane	UiO-66-NH <sub>2</sub>			440	47		
	PIM-grafted-UiO-66-NH <sub>2</sub>	1	CO <sub>2</sub> /N <sub>2</sub>	247	56	30 °C, 1 bar, SG	Husna et al. (2022)
	UiO-66-IL-ClO <sub>4</sub>	50	CO <sub>2</sub> /N <sub>2</sub>	3GPU	32	25 °C, 6 bar, MG	Yao et al. (2017)
Matrimid 5218 Pebax 1657	Bipyridine-based UiO-67	10	CO <sub>2</sub> /CH <sub>4</sub>	26	75	30 °C, 5 bar, MG	Thür et al. (2019)
	UiO-66@IL	30	CO <sub>2</sub> /N <sub>2</sub>	143	61	25 °C, 10 bar, SG	Iqbal et al. (2022)
Pebax 1657	UiO-66-(OH) <sub>2</sub> @PIL	20	CO <sub>2</sub> /N <sub>2</sub>	132	71	25 °C, 2 bar, SG	Yang et al. (2022)
	UiO-66-(OH) <sub>2</sub>	5		128	59		
PIM-1	Ag <sup>+</sup> @UiO-66-NH <sub>2</sub>	30	CO <sub>2</sub> /N <sub>2</sub>	15000	30	25 °C, 2 bar, MG	Lin et al. (2023)
PIM-1	UiO-66-(CF <sub>3</sub> ) <sub>2</sub>	8	CO <sub>2</sub> /N <sub>2</sub>	5242	34	60 °C, 1 bar, SG	Zhou et al. (2024)
PIM-1	UiO-66	7.5	CO <sub>2</sub> /CH <sub>4</sub>	8995	13	35 °C, 3 bar, MG	Yahia et al. (2024)
PIM-1	UiO-66	15	CO <sub>2</sub> /N <sub>2</sub>	7212	26	30 °C, 1 bar, SG	Wang et al. (2024)
PVDF	UiO-66-NM@PEG	18.75	CO <sub>2</sub> /N <sub>2</sub>	538	48	25 °C, 1 bar, SG	Li et al. (2023)
PDMS				724	21		
Pebax				307	31		
PIM-PU	UiO-66-NH <sub>2</sub>	10	CO <sub>2</sub> /N <sub>2</sub>	333	138	35 °C, 1 bar, SG	Fan et al. (2022)
Cellulose	UiO-66	10	CO <sub>2</sub> /CH <sub>4</sub>	257	71	85 °C, 3 bar, SG	Jia et al. (2024)
Pebax 1657	CS-UiO-66-NH <sub>2</sub>	5	CO <sub>2</sub> /CH <sub>4</sub>	590	41	25 °C, 2 bar, SG	Wang et al. (2024)
Pebax 1657	CeZrUiO66-NH <sub>2</sub>	3	CO <sub>2</sub> /N <sub>2</sub>	101	76	35 °C, 1 bar, SG	Du et al. (2023)

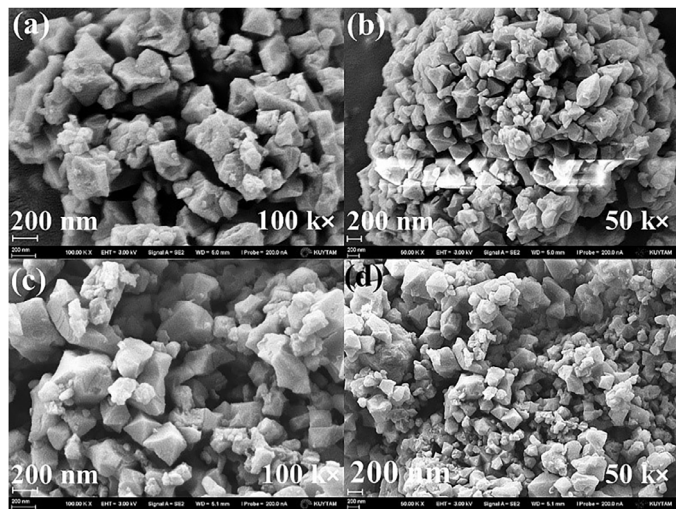


Fig. 5. SEM images of (a, b) MIL-101(Cr) and (c, d) [MPPyr][DCA]/MIL-101(Cr) composite (Habib et al., 2023). Reprinted with permission from Elsevier. Copyright 2023.

face area and total pore volume of MIL-101(Cr) decreased after the ionic liquid modification, which resulted from the pore occupation with ionic liquid. The synthesized composite showed much higher CO<sub>2</sub> adsorption capacity than the pristine MIL-101(Cr). As a result, the manufactured MMMs with modified MIL-101(Cr) had a much higher CO<sub>2</sub> separation efficiency.

Sasikumar and Arthanareeswaran (2022) synthesized MIL-53(Al) and modified it with ionic liquid (IL) [bmim][NTf<sub>2</sub>] by using the post-

synthetic modification strategy to improve the compatibility between MIL-53(Al) filler and polysulfone (PSf) matrix. The IL@ MIL-53(Al)/PSf MMMs were prepared by using the solution casting and phase inversion method. The crystal structure of MIL-53(Al) was perfectly preserved after the IL modification. The mechanical stability of membranes was enhanced owing to the enhanced compatibility between fillers and polymer chains. The maximum CO<sub>2</sub>/N<sub>2</sub> selectivity of 31 and CO<sub>2</sub>/CH<sub>4</sub> of 28, as well as the highest CO<sub>2</sub> permeance of 34 GPU, were found in MMMs having 2 wt% IL@MIL-53(Al).

As presented in Table 3, MIL-101, MIL-53, MIL101-NH<sub>2</sub> and MIL53-NH<sub>2</sub> are generally used MIL-type MOFs for the fabrication of CO<sub>2</sub> selective MMMs. Pebax, PIM-1, PSf, PVDF, Tröger's base polymer, cellulose acetate, and polyimide are used as polymer matrix. The filler content is between 4 wt% and 20 wt%. It can be found the MMMs containing modified MIL MOFs showed higher separation efficiency of CO<sub>2</sub> molecules than MMMs containing pristine MIL MOFs.

#### 2.4. MMMs containing other types of MOFs

In addition to the abovementioned ZIFs, UiOs, and MILs, various types of other MOFs have been synthesized and utilized in the fabrication of CO<sub>2</sub> selective MMMs. Table 4 has summarized the CO<sub>2</sub>/N<sub>2</sub> and CO<sub>2</sub>/CH<sub>4</sub> separation properties of MMMs containing other types of MOFs. Among these various types of MOFs, the selected examples will be discussed and summarized in the following sections.

Chuah et al. (2019) modified HKUST-1 by using the post-synthetic method. The synthesized HKUST-1 was modified with 3-picolyamine. Subsequently, modified HKUST-1/Matrimid MMMs were fabricated. It was found that the BET surface area and the total micropore volume decreased after amine modification. The prepared MMMs containing 20 wt% amine modified HKUST-1 showed 25 % higher CO<sub>2</sub> perme-

**Table 3**Summary of separation efficiency of CO<sub>2</sub> molecules of MMMs containing MIL MOFs (SG - single gas, MG - mixed gas).

Polymers	MOFs	MOF content [wt%]	Gas pairs	P <sub>CO<sub>2</sub></sub> [Barrer]	Selectivity	Testing conditions	Refs.
6FDA-durene	NH <sub>2</sub> -MIL-125 (Ti)	7	CO <sub>2</sub> /CH <sub>4</sub>	1116	37	25 °C, 3.5 bar, SG	Suhaimi et al. (2020)
Pebax-1657	MIL-101	15	CO <sub>2</sub> /N <sub>2</sub>	28	89	-20 °C, 3.5 bar, SG	Song et al. (2020)
Pebax-1657	NH <sub>2</sub> -MIL-101	5	CO <sub>2</sub> /N <sub>2</sub>	30	96	-20 °C, 2 bar, SG	Song et al. (2020)
PIM-1	MIL-53	4	CO <sub>2</sub> /CH <sub>4</sub>	953	13	30 °C, 0.5 bar, SG	Aliyev et al. (2021)
	MIL-53	4	CO <sub>2</sub> /N <sub>2</sub>	953	17		
PIM-EA-TB	MIL-101(Cr)	25	CO <sub>2</sub> /CH <sub>4</sub>	10000	11	35 °C, 1 bar, SG	Esposito et al. (2024)
	MIL-177(Ti)			7000	11		
Pebax-1657	Azo@NH <sub>2</sub> -MIL-53	20	SO <sub>2</sub> /N <sub>2</sub>	2570 (SO <sub>2</sub> )	717	35 °C, 2 bar, MG	Xin et al. (2022)
Ultem®1000	APTMS modified MIL-53	15	CO <sub>2</sub> /N <sub>2</sub>	31 GPU	36	35 °C, 25 bar, SG	Zhu et al. (2018)
Cellulose acetate	NH <sub>2</sub> -MIL-53(Al)	15	CO <sub>2</sub> /CH <sub>4</sub>	2.9 GPU	12	30 °C, 3 bar, MG	Mubashir et al. (2020)
Tröger's base polymer	NH <sub>2</sub> -MIL-53 (Al)	20	CO <sub>2</sub> /N <sub>2</sub>	325	20	35 °C, 4 bar, SG	Fan et al. (2019)
			CO <sub>2</sub> /CH <sub>4</sub>	325	19		
PVDF	NH <sub>2</sub> -MIL-125 (Ti)	2	CO <sub>2</sub> /CH <sub>4</sub>	822 GPU	8	25 °C, 2 bar, SG	Ding et al. (2023)
PGO/PSf	MIL-140C	20	CO <sub>2</sub> /N <sub>2</sub>	1768 GPU	38	25 °C, 1 bar, SG	Kang et al. (2022)
Pebax-3533	MIL-178(Fe)	5	CO <sub>2</sub> /N <sub>2</sub>	312	25	35 °C, 1 bar, MG	Hasan et al. (2022)
PSf	[bmim][NTf <sub>2</sub> ]@ MIL-53	2	CO <sub>2</sub> /N <sub>2</sub>	34 GPU	31	30 °C, 4 bar, SG	Sasikumar & Arthanareeswaran, 2022
			CO <sub>2</sub> /CH <sub>4</sub>		28		
Pebax-1657	[MPPyr][DCA]@ MIL-101(Cr)	15	CO <sub>2</sub> /CH <sub>4</sub>	148	122	35 °C, 1 bar, SG	Habib et al. (2023)
			CO <sub>2</sub> /N <sub>2</sub>	148	1348		

**Table 4**Separation efficiency of CO<sub>2</sub> molecules of MMMs containing other types of MOFs (SG - single gas, MG - mixed gas).

Polymers	MOFs	MOF content [wt%]	Gas pairs	P <sub>CO<sub>2</sub></sub> [Barrer]	Selectivity	Testing conditions	Refs.
PIM-1	Mg-MOF-74	8	CO <sub>2</sub> /CH <sub>4</sub>	1935	12	30 °C, 0.5 bar, SG	Aliyev et al. (2021)
	Mg-MOF-74	8	CO <sub>2</sub> /N <sub>2</sub>	1935	17		
	TIFSIX-3	4	CO <sub>2</sub> /CH <sub>4</sub>	1000	14		
	TIFSIX-3	4	CO <sub>2</sub> /N <sub>2</sub>	1000	19		
PIM-1	MUF-15	15	CO <sub>2</sub> /N <sub>2</sub>	23000	15	20 °C, 1 bar, SG	Yin et al. (2020)
PIM-1	MOF-801	5	CO <sub>2</sub> /N <sub>2</sub>	9686	27	35 °C, 4 bar, SG	Chen et al. (2020)
PIM-1	MOF-808	10	CO <sub>2</sub> /CH <sub>4</sub>	9090	16	35 °C, 3 bar, MG	Yahia et al. (2024)
PIM-1	MOF-303	30	CO <sub>2</sub> /CH <sub>4</sub>	7528	28	35 °C, 2 bar, MG	Chen et al. (2023)
PIM-1	[Bmim][NTf <sub>2</sub> ]@MOF-801	5	CO <sub>2</sub> /N <sub>2</sub>	9420	29	35 °C, 4 bar, SG	Chen et al. (2021)
PS	Bio-MOF-1	30	CO <sub>2</sub> /CH <sub>4</sub>	17	43	25 °C, 10 bar, SG	Ishaq et al. (2019)
			CO <sub>2</sub> /N <sub>2</sub>	17	46		
PVAc	Mg-MOF-74	20	CO <sub>2</sub> /CH <sub>4</sub>	5	25	25 °C, 6 bar, MG	Majumdar et al. (2020)
PTO/PTMSP/PSf	UTSA-16	10	CO <sub>2</sub> /N <sub>2</sub>	1070 GPU	41	30 °C, 1 bar, SG	Min et al. (2023)
			CO <sub>2</sub> /CH <sub>4</sub>	17			
Pebax-1657	NOTT-300	40	CO <sub>2</sub> /N <sub>2</sub>	395	61	25 °C, 10 bar, SG	Habib et al. (2020)
			CO <sub>2</sub> /CH <sub>4</sub>	36			
Matrimid	La-BTC	30	CO <sub>2</sub> /N <sub>2</sub>	21	48	25 °C, 10 bar, SG	Bano et al. (2022)
			CO <sub>2</sub> /CH <sub>4</sub>	55			
Matrimid	ZnO@ZnBDC	0.75	CO <sub>2</sub> /CH <sub>4</sub>	12	40	35 °C, 1 bar, SG	Li et al. (2022)
6FDA-DAM:DABA	CAU-10-H	25	CO <sub>2</sub> /CH <sub>4</sub>	29	67	35 °C, 2 bar, SG	Yu et al. (2022)
Matrimi® 5218	MOF [Co(AzDC)]	10	CO <sub>2</sub> /N <sub>2</sub>	156	78	30 °C, 1 bar, MG	Xin et al. (2022)
Matrimid®	HKUST-1-25NH <sub>2</sub>	20	CO <sub>2</sub> /N <sub>2</sub>	13	43	35 °C, 1 bar, MG	Chuah et al. (2019)
6FDA-durene	HKUST-Emin[Tf <sub>2</sub> N]	10	CO <sub>2</sub> /N <sub>2</sub>	1102	27	25 °C, 2 bar, SG	Lin et al. (2016)
		10	CO <sub>2</sub> /CH <sub>4</sub>	1102	29		
PSf	Cu-BTC/[Dmim][Cl]	1	CO <sub>2</sub> /N <sub>2</sub>	29 GPU	26	30 °C, 4 bar, SG	Sasikumar & Arthanareeswaran, 2022
			CO <sub>2</sub> /CH <sub>4</sub>	24			
Pebax 1657	Gly@CuBTC	5	CO <sub>2</sub> /CH <sub>4</sub>	175	29	25 °C, 20 bar, SG	Wu et al. (2022)
	CuBTC	3		165	23		
	Gly@CuBTC	5		175	32	25 °C, 20 bar, MG	
PEI	HKUST-1	50	CO <sub>2</sub> /CH <sub>4</sub>	28	6	25 °C, 1.5 bar, SG	Wang et al. (2022)
PVAm	MOF-808@PVAm	33.33	CO <sub>2</sub> /N <sub>2</sub>	399	181	25 °C, 3 bar, MG	Ge et al. (2024)

ability and 38 % higher CO<sub>2</sub>/N<sub>2</sub> selectivity comparing with the pristine Matrimid membranes. This is because the amine-modified HKUST-1 could suppress the diffusivity and solubility of N<sub>2</sub> but increase the diffusivity of CO<sub>2</sub> significantly.

Majumdar et al. (2020) synthesized Mg-MOF-74 and fabricated MMMs for CO<sub>2</sub>/CH<sub>4</sub> separation by incorporating Mg-MOF-74 into polyvinyl acetate (PVAc) matrix. The synthesized Mg-MOF-74 showed a strong interaction with CO<sub>2</sub> molecules while a rather weak interaction with CH<sub>4</sub> molecules, which is revealed by the high CO<sub>2</sub> adsorption capacity of 20.6 cm<sup>3</sup>/g and the low CH<sub>4</sub> adsorption capacity of 2.0 cm<sup>3</sup>/g. The MMMs showed much greater CO<sub>2</sub> permeability and CO<sub>2</sub>/CH<sub>4</sub> se-

lectivity when compared to the pristine membranes. This is explained by the Mg-MOF-74 crystals' high porosity, strong CO<sub>2</sub> adsorption affinity, and uniform distribution throughout the PVAc matrix. Moreover, the CO<sub>2</sub> permeability and CO<sub>2</sub>/CH<sub>4</sub> selectivity were barely changed at high pressure, indicating that the plasticization effect of polymeric membranes was significantly inhibited due to the incorporation of Mg-MOF-74 crystals.

Chen et al. (2021) modified MOF-801 with [bmim][Tf<sub>2</sub>N] via wet impregnation because [bmim][Tf<sub>2</sub>N] possesses high CO<sub>2</sub> affinity. Subsequently, the [bmim][Tf<sub>2</sub>N]@MOF-801 nanocomposite was incorporated into the PIM matrix to prepare MMMs with enhanced gas separa-

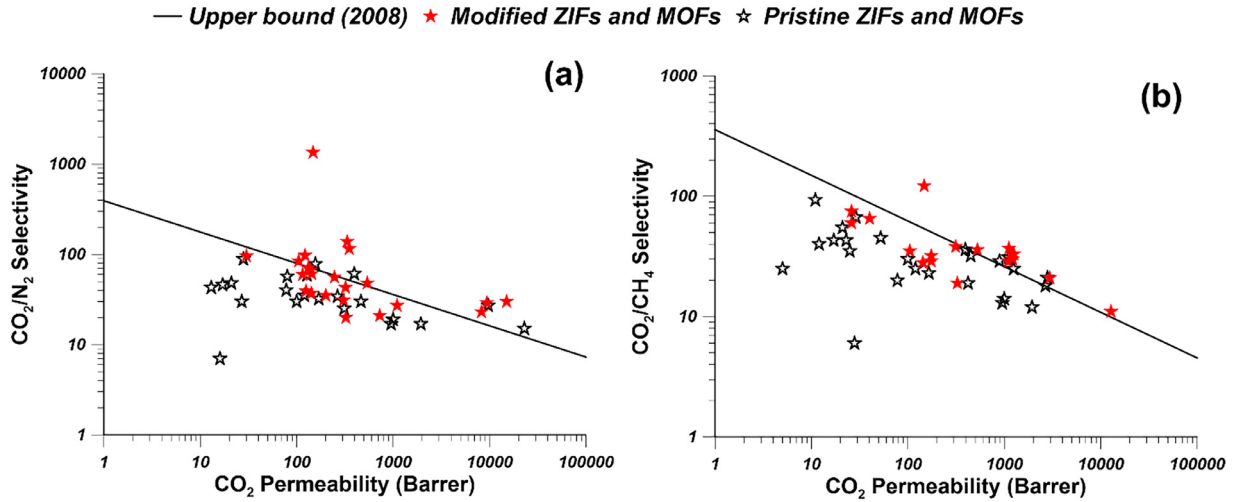


**Fig. 6.** The comparison of (a) CO<sub>2</sub>/N<sub>2</sub> separation performance and (b) CO<sub>2</sub>/CH<sub>4</sub> separation performance of MMMs containing pristine MOFs and functionalized MOFs (data are from Tables 1–4).

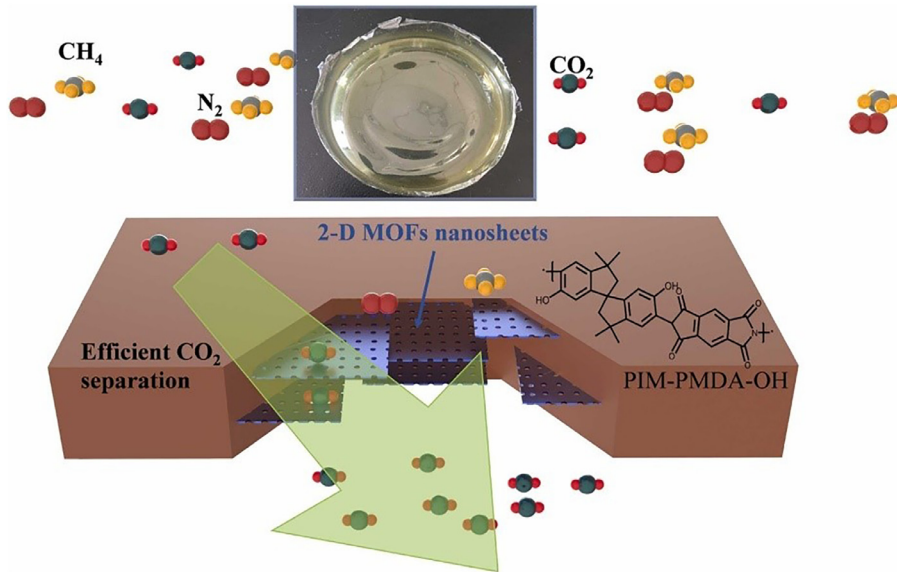


**Fig. 7.** Schematic illustration of 2-D MOFs/PIM-PMDA-OH MMMs (Ma et al., 2022). Reprinted with permission from Elsevier. Copyright 2022.

ration performance. MMMs containing 5 wt% of [bmim][Tf<sub>2</sub>N]@MOF-801 exhibited 129 % higher CO<sub>2</sub> permeability (9420 Barrer) and 45 % higher CO<sub>2</sub>/N<sub>2</sub> selectivity (29), comparing with pristine PIM-1 membranes. This is because more active sites in [bmim][Tf<sub>2</sub>N]@MOF-801 were exposed, resulting in the improvement of CO<sub>2</sub> adsorption since [bmim][Tf<sub>2</sub>N]@MOF-801 could be well dispersed in the polymer matrix. MMMs showed desirable anti-plasticization and anti-aging features due to the good chemical stability of [bmim][Tf<sub>2</sub>N]@MOF-801.

Tables 1–4 summarize the CO<sub>2</sub> separation efficiency of MMMs containing ZIFs and MOFs. Various types of ZIFs and MOFs were synthesized and used as fillers in MMMs for CO<sub>2</sub> separation, such as UiO, ZIF, HKUST, and MIL. These MOFs used for CO<sub>2</sub> separation usually possess relatively high BET surface area, high CO<sub>2</sub> adsorption capacity, ease of functionalization, and size-sieving effects. According to the aforementioned discussion and data gathered in Table 1–4, MOFs could be directly incorporated into a polymer matrix for the fabrication of MMMs for gas separation. This is because MOFs could increase the gas permeability without decreasing the gas selectivity, owing to its porous structure and high affinity to CO<sub>2</sub> molecules. Moreover, the material properties of MMMs were also enhanced. For example, the MMMs usually possess high mechanical and thermal stability and good anti-aging and anti-plasticization properties. In order to further enhance the com-

patibility between MOFs and polymer chains and obtain a more homogeneous distribution of MOFs in a polymer matrix, MOFs could be modified by using the *in situ* modification method (Wang et al., 2020; Thür et al., 2019) and the post-synthetic modification method (Liu et al., 2020; Chuah et al., 2019). The surface modification also tunes the pore size, surface area, and the CO<sub>2</sub> affinity of MOFs. As a result, the fabricated MMMs possess a uniform distribution of MOFs and enhanced CO<sub>2</sub> separation efficiency.

The comparison between Robeson upper bound 2008 and the CO<sub>2</sub> separation efficiency of MMMs containing ZIFs or MOFs is presented in Fig. 6. It was found that the utilization of ZIFs and MOFs could significantly improve the CO<sub>2</sub> separation efficiency of MMMs since their performance was either close to or over the Robeson upper bound 2008. However, the MMMs containing modified ZIFs or MOFs showed higher CO<sub>2</sub> separation efficiency, indicating that the modification of ZIFs and MOFs is a promising way to enhance the CO<sub>2</sub> separation efficiency of MMMs.

### 3. 2D materials as fillers in MMMs

2D materials have shown intriguing properties in the fabrication of MMMs for CO<sub>2</sub> separation due to their nanometer thickness, layered

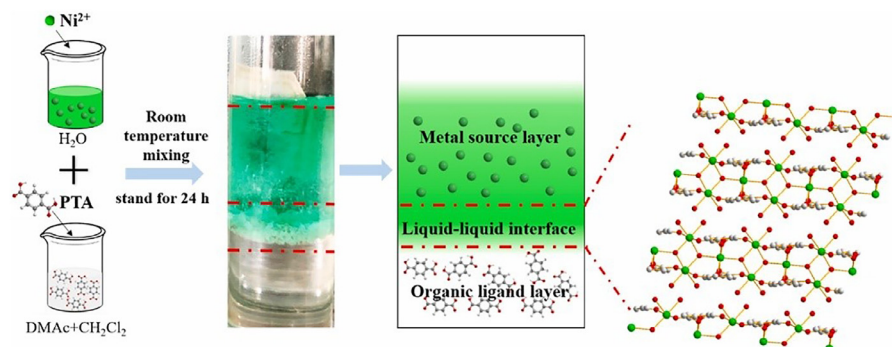


**Fig. 8.** Illustration of the synthesis of Ni-MOFs by using the liquid-liquid interface synthesis method (Zhu et al., 2023). Reprinted with permission from Elsevier. Copyright 2023.

**Table 5**  
Separation efficiency of CO<sub>2</sub> molecules of MMMs containing 2D MOFs (SG - single gas, MG - mixed gas).

Polymers	2D MOFs	Filler content [wt%]	Gas pairs	P <sub>CO<sub>2</sub></sub> [Barrer]	Selectivity	Testing conditions	Refs.
Pebax 1657	CuBDC-ns@MoS <sub>2</sub>	2.5	CO <sub>2</sub> /N <sub>2</sub>	123	69	35 °C, 4 bar, SG	Liu et al. (2022)
			CO <sub>2</sub> /CH <sub>4</sub>	18			
			CO <sub>2</sub> /N <sub>2</sub>	108	50	35 °C, 4 bar, MG	
			CO <sub>2</sub> /CH <sub>4</sub>	110	13		
Pebax 1657	ZIF-67 nanosheets	5	CO <sub>2</sub> /N <sub>2</sub>	139	73	25 °C, 1 bar, SG	Feng et al. (2020)
				118	58	25 °C, 1 bar, MG	
Pebax 1657	Cu(BPY) <sub>2</sub> (OTF) <sub>2</sub>	4	CO <sub>2</sub> /CH <sub>4</sub>	84	14	25 °C, 1 bar, MG	Gou et al. (2021)
Polyimide	C-axis oriented ZIF-95 sheets	40	H <sub>2</sub> /CO <sub>2</sub>	967 (H <sub>2</sub> )	58	100 °C, 1 bar, SG	Pang et al. (2023)
Polyimide	ZIF-L	45	H <sub>2</sub> /CO <sub>2</sub>	369 (H <sub>2</sub> )	19	25 °C, 1.5 bar, MG	Jia et al. (2024)
PIM-1	BCoC-ZIF	10	CO <sub>2</sub> /N <sub>2</sub>	7326	33	25 °C, 2 bar, MG	Sun et al. (2022)
PIM-1	NUS-8-NH <sub>2</sub>	10	CO <sub>2</sub> /N <sub>2</sub>	14638	29	25 °C, 2 bar, MG	Pu et al. (2022)
PIM-1	MUF-15 nanosheets	5	CO <sub>2</sub> /N <sub>2</sub>	16000	20	20 °C, 1 bar, SG	Yin et al. (2020)
Tröger's base polymer	ZIF-L-Zn	20	CO <sub>2</sub> /N <sub>2</sub>	475	13	24 °C, 2 bar, SG	Deng et al. (2020)
			CO <sub>2</sub> /CH <sub>4</sub>		12		
	ZIF-L-Co		CO <sub>2</sub> /N <sub>2</sub>	552	12		
			CO <sub>2</sub> /CH <sub>4</sub>		11		
Pebax 1657	Ni-MOF nanosheets	6	CO <sub>2</sub> /CH <sub>4</sub>	436	33	25 °C, 2 bar, MG	Zhu et al. (2023)
PIM-PMDA-OH	Zn <sub>2</sub> (bim) <sub>4</sub> nanosheets	22	CO <sub>2</sub> /N <sub>2</sub>	342	55	35 °C, 1 bar, SG	Ma et al. (2022)
			CO <sub>2</sub> /CH <sub>4</sub>		49		
			CO <sub>2</sub> /N <sub>2</sub>	173	58	35 °C, 1 bar, MG	
			CO <sub>2</sub> /CH <sub>4</sub>		54		
Pebax 1657	ZIF-67-L	10	CO <sub>2</sub> /N <sub>2</sub>	92	52	30 °C, 2 bar, SG	Zhao et al. (2023)
Pebax 1657	2D ZIF-8	10	CO <sub>2</sub> /N <sub>2</sub>	350	94	25 °C, 2 bar, SG	Jeong et al. (2024)
Pebax-3533	PEI-ZIF-L	2	CO <sub>2</sub> /N <sub>2</sub>	639	27	35 °C, 2 bar, MG	Qin et al. (2024)
Pebax-3533	PAMAM-ZIF-L			703	24		
PEGMEA	SUM-9	1	CO <sub>2</sub> /N <sub>2</sub>	539	25	35 °C, 2 bar, SG	Feng et al. (2023)
	Cu-TCPP	0.1	CO <sub>2</sub> /N <sub>2</sub>	1183	76	25 °C, 1.5 bar, SG	Wang et al. (2023)
PIM-1	NUS-8-COOH	2	CO <sub>2</sub> /N <sub>2</sub>	10400	31	25 °C, 2 bar, MG	Wang et al. (2022)
Pebax 1657	MFI	5	CO <sub>2</sub> /CH <sub>4</sub>	11050	14		
			CO <sub>2</sub> /CH <sub>4</sub>	190	30	25 °C, 2 bar, MG	Zhang et al. (2021)

sheet structure, and micro-scale lateral dimensions (Dai et al., 2023). Generally, the atomic layered 2D nanosheets have a large amount of exposed surface atoms and active sites. Moreover, the edge effects of 2D nanosheets can also enhance their chemical activity. The adjustable space between layers, the unique properties, the feasibility of surface modification, and the lateral structure of 2D nanosheets provide special performance in transporting and separating molecules in membrane processes (Duan et al., 2019). For example, when gas molecules are transported through MMMs containing graphene oxide (GO) nanosheets, the gas molecules transporting pathways can be effectively regulated. The 2D nanosheets align parallel to the membrane surface, creating distorted diffusion pathways for larger gas molecules (CH<sub>4</sub> and N<sub>2</sub>) and enhancing their transporting resistance. The interlayer spacing between 2D nanosheets created highly selective and permeable 2D nanochannels for smaller gas molecules (CO<sub>2</sub>) (Shi et al., 2021). As a result, MMMs containing 2D materials showed enhanced CO<sub>2</sub>/N<sub>2</sub> and CO<sub>2</sub>/CH<sub>4</sub> separation performance. Therefore, the synthesis and modification of 2D materials such as 2D MOFs, 2D carbon-based materials, and MXene

and their applications in MMMs for CO<sub>2</sub> separation is discussed in this section.

### 3.1. MMMs containing 2D MOFs

2D MOFs combine the advantages of both MOFs and 2D nanosheets, e.g., the high surface area, the short diffusion path, the tunable structure, the high amount of exposed active sites, the unique molecular arrays, and the ordered porous structures (Duan et al., 2019; Ma et al., 2022). 2D MOFs show great potential in nanotechnology applications that cannot be fulfilled by using other 2D materials and 3D MOFs (Duan et al., 2019). In particular, 2D MOFs can improve the phase integration and filler orientation of polymer matrix, resulting in a significant improvement in CO<sub>2</sub> separation efficiency (Weng et al., 2016).

Ma et al. (2022) synthesized 2D MOF Zn<sub>2</sub>(bim)<sub>4</sub> via hydrothermal transformation of ZIF-7 in boiling water. Subsequently, PIM-PMDA-OH/2D MOF MMMs were prepared for CO<sub>2</sub> separation (Fig. 7). The MOF nanosheets were homogeneously distributed in a polymer matrix with-

out defects inside the MMMs. The high compatibility of MOF nanosheets has resulted from the hydrogen bond between the amino groups from the benzimidazole ligand and the hydroxyl groups from the polymer matrix. The high CO<sub>2</sub> permeability was attributed to the higher free volume and short diffusion path ways for CO<sub>2</sub> molecules provided by the porous 2D MOFs nanosheets. However, the lateral size of 2D MOFs nanosheets forced the bigger molecules N<sub>2</sub> and CH<sub>4</sub> to travel in a tortuous pathway, resulting in increased transport resistance. Therefore, the CO<sub>2</sub> separation efficiency of MMMs was enhanced owing to the excellent molecular sieving effects and chemical stability of 2D MOF Zn<sub>2</sub>(bim)<sub>4</sub>.

Besides the preparation of 2D MOFs from bulk MOFs, Zhu et al. (2023) synthesized a 2D layered Ni-MOF ([Ni<sub>3</sub>(OH)<sub>2</sub>(1,4-BDC)<sub>2</sub>(H<sub>2</sub>O)<sub>4</sub>] 2H<sub>2</sub>O) by using the liquid-liquid interface synthesis method (Fig. 8). The interlayer distance of the layered-structure Ni-MOF was 0.928 nm. Moreover, the defective Ni-MOF was also synthesized by controlling the molar ratio of metal ions to the organic linker. The defective Ni-MOF possessed a larger pore size than that of pristine Ni-MOF, which allowed easier transport of CO<sub>2</sub> molecules. The defective Ni-MOF nanosheets were homogeneously distributed in the Pebax 1657 matrix owing to their good compatibility with the polymer matrix. Comparing with the pristine membranes, MMMs with 6 wt% of defective Ni-MOF showed 115 % higher CO<sub>2</sub> permeability and 18 % higher selectivity. The enhanced CO<sub>2</sub> separation efficiency resulted from the increased polymer chain spacing, the low mass transfer resistance resulted from the mesoporous structure of defective Ni-MOF, and the enhanced interaction between CO<sub>2</sub> molecules and the active metal sites from defective Ni-MOF.

Table 5 summarizes the separation efficiency of CO<sub>2</sub> molecules of MMMs containing 2D MOFs. It can be found that ZIF-based 2D MOFs are the most studied fillers in MMMs for gas separation. In addition to ZIF-based 2D MOFs, 2D MOFs, such as CuBDC nanosheets (Liu et al., 2022), Cu(BPY)<sub>2</sub>(OTF)<sub>2</sub> (Gou et al., 2021), NUS-8-NH<sub>2</sub> (Pu et al., 2022),

MUF-15 nanosheets (Yin et al., 2020) and SUM-9 (Feng et al., 2023) were also synthesized and used as fillers for MMMs fabrication. Except in some cases, the low content ( $\leq 10$  wt%) of 2D MOFs in MMMs showed significant improvement in the gas separation efficiency owing to their unique properties and advantages. 2D MOFs are promising in the fabrication of MMMs for gas separation.

### 3.2. MMMs containing 2D carbon-based materials

The 2D layered material graphene and graphene oxide (GO) were used to fabricate membranes for various separation processes due to their tunable surface chemistry and the feasibility of preparation. For example, GO contains many chemical groups, e.g., carboxyl, epoxy, hydroxyl, and carbonyl groups, which improve the affinity to CO<sub>2</sub> molecules. Moreover, the high aspect ratio of GO can regulate the gas transport pathways, which increases the diffusivity selectivity of gas molecules (Dai et al., 2023). Graphite carbon nitride (g-C<sub>3</sub>N<sub>4</sub>) is also attractive in the preparation of membranes due to its special physico-chemical features, high chemical stability, and thin layered structure. The structure unit of g-C<sub>3</sub>N<sub>4</sub> consists of 6-membered rings connected by the sp<sup>2</sup> hybridization of C and N atoms (Cui et al., 2018). Moreover, the pore size of g-C<sub>3</sub>N<sub>4</sub> is in the range of 0.31 nm–0.34 nm, which is bigger than the kinetic diameter of hydrogen and carbon dioxide but smaller than that of other gas molecules. As a result, g-C<sub>3</sub>N<sub>4</sub> possesses great potential in preparing membranes for gas separation (Dai et al., 2023).

Chen et al. (2022) modified GO with amino acids, e.g., cysteine, arginine, and histidine via crosslinking. Subsequently, MMMs containing modified GO were fabricated for CO<sub>2</sub> separation. All the amino acids were grafted on the GO, and the loading content was more than 20 %. Comparing with GO/Pebax MMMs, modified GO showed more homo-

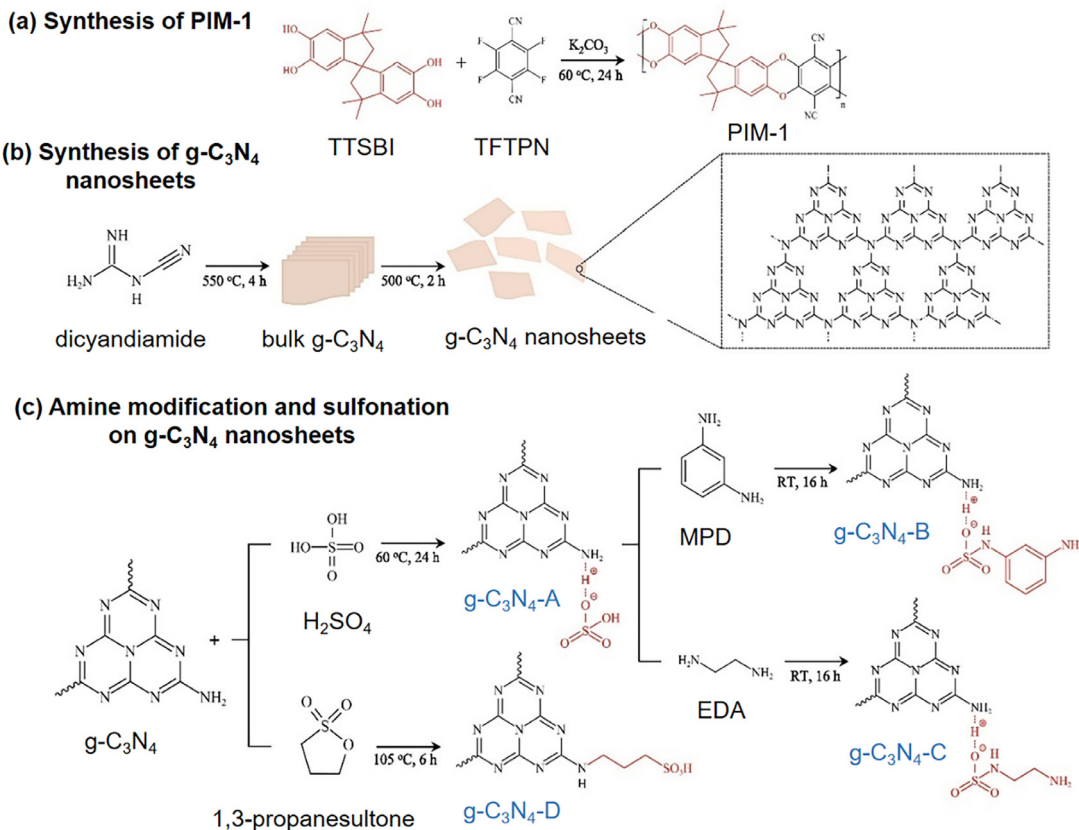


Fig. 9. Synthesis of (a) PIM-1, (b) g-C<sub>3</sub>N<sub>4</sub> nanosheets, and (c) amine modification and sulfonation on g-C<sub>3</sub>N<sub>4</sub> nanosheets (Voon et al., 2022). Reprinted with permission from Elsevier. Copyright 2022.

**Table 6**Separation efficiency of CO<sub>2</sub> molecules of MMMs containing 2D carbon-based fillers (SG - single gas, MG - mixed gas).

Polymers	2D carbon-based materials	Filler content [wt%]	Gas pairs	P <sub>CO<sub>2</sub></sub> [Barrer]	Selectivity	Testing conditions	Refs.
POEM	GO-GMA	-	CO <sub>2</sub> /N <sub>2</sub> CO <sub>2</sub> /CH <sub>4</sub>	3169 GPU 16	37 16	25 °C, 1 bar, SG	Lee et al. (2023)
Pebax 1657	Arginine@GO Histidine@GO	0.4	CO <sub>2</sub> /N <sub>2</sub>	169 149	70 50	25 °C, 1 bar, SG	Chen et al. (2022)
PIM-1	GO-POSS	0.05	CO <sub>2</sub> /N <sub>2</sub> CO <sub>2</sub> /CH <sub>4</sub>	12000 13944	20 14	25 °C, 1 bar, SG	Mohsenpour et al. (2022)
Pebax 1657	2D MCNs	0.5	CO <sub>2</sub> /N <sub>2</sub> CO <sub>2</sub> /CH <sub>4</sub>	123 20	76 61	25 °C, 4 bar, SG	Yang et al. (2021)
Pebax 2533	GO	0.02	CO <sub>2</sub> /N <sub>2</sub>	400	25	25 °C, 4 bar, MG	Casadei et al. (2020)
Pebax 1657/PAN	g-C <sub>3</sub> N <sub>4</sub> nanosheets	0.25	CO <sub>2</sub> /N <sub>2</sub>	33 GPU	68	35 °C, 1 bar, MG 25 °C, 3 bar, SG	Cheng et al. (2020)
PIM-1	APTS-GO	0.5	CO <sub>2</sub> /CH <sub>4</sub>	5600	12	25 °C, 1.5 bar, MG	Luque-Alled et al. (2021)
Matrimid® 5218	Nitrogen-doped graphene	0.07	CO <sub>2</sub> /N <sub>2</sub>	10 GPU	42	35 °C, 1 bar, MG	Yang et al. (2020)
PEEK	Sulfonated polymer brush modified GO	8	CO <sub>2</sub> /N <sub>2</sub> CO <sub>2</sub> /CH <sub>4</sub>	1300 73	88 73	25 °C, 1 bar, SG	Xin et al. (2019)
Pebax 1657/PSf	A-prGO	0.1	CO <sub>2</sub> /N <sub>2</sub> CO <sub>2</sub> /CH <sub>4</sub>	48 24	106 24	25 °C, 4 bar, SG	Mohammed et al. (2019)
Pebax 1657	APTS-GO	0.9	CO <sub>2</sub> /N <sub>2</sub> CO <sub>2</sub> /CH <sub>4</sub>	934 910	71 41	35 °C, 2 bar, MG	Zhang et al. (2019)
Pebax 1657	GO-mPD	0.7	CO <sub>2</sub> /N <sub>2</sub>	30	142	25 °C, 4 bar, SG	Mehdinia Lichaei et al. (2022)
Pebax 1657	GO	1	CO <sub>2</sub> /N <sub>2</sub>	114	69	30 °C, 2 bar, SG	Shi et al. (2021)
Pebax 1657	GO	1	CO <sub>2</sub> /N <sub>2</sub>	56	121	25 °C, 4 bar, SG	Pazani & Aroujalian, 2020
PVDF	GO	0.5	CO <sub>2</sub> /N <sub>2</sub>	1	41	27 °C, 5 bar, SG	Feijani et al. (2018)
PIM-1	Sulfonated g-C <sub>3</sub> N <sub>4</sub>	1	CO <sub>2</sub> /N <sub>2</sub> CO <sub>2</sub> /CH <sub>4</sub>	3740 12	20 12	35 °C, 3.5 bar, SG	Voon et al. (2022)

**Table 7**Separation efficiency of CO<sub>2</sub> molecules of MMMs containing MXene (SG - single gas, MG - mixed gas).

Polymers	MXene	Filler content [wt%]	Gas pairs	P <sub>CO<sub>2</sub></sub> [Barrer]	Selectivity	Testing conditions	Refs.
PEG-600	Ti <sub>3</sub> C <sub>2</sub> T <sub>x</sub>	75	CO <sub>2</sub> /N <sub>2</sub> CO <sub>2</sub> /CH <sub>4</sub> CO <sub>2</sub> /N <sub>2</sub> CO <sub>2</sub> /CH <sub>4</sub>	814 28 956 27	32 31	25 °C, 1 bar, SG	Luo et al. (2022)
Pebax 1657/PAN	Ti <sub>3</sub> C <sub>2</sub> T <sub>x</sub>	0.15	CO <sub>2</sub> /N <sub>2</sub>	22 GPU	73	25 °C, 1 bar, MG	Liu et al. (2020)
Pebax 1657	Ti <sub>3</sub> C <sub>2</sub> T <sub>x</sub>	10	CO <sub>2</sub> /N <sub>2</sub>	584	59	30 °C, 2 bar, SG	Shi et al. (2021)
Pebax 1657	Ti <sub>3</sub> C <sub>2</sub> T <sub>x</sub>	0.05	CO <sub>2</sub> /N <sub>2</sub> CO <sub>2</sub> /CH <sub>4</sub>	1987 GPU 15	42	25 °C, 4 bar, SG	Shamsabadi et al. (2020)
PDMS	Ti <sub>3</sub> C <sub>2</sub> T <sub>x</sub>	1	CO <sub>2</sub> /N <sub>2</sub>	13917	14	35 °C, 1 bar, MG	Ahmad et al. (2023)
Pebax 1657	Ti <sub>3</sub> C <sub>2</sub> T <sub>x</sub>	1	CO <sub>2</sub> /N <sub>2</sub>	148	63	30 °C, 2 bar, SG	Shi et al. (2021)
Pebax 1657	Ti <sub>3</sub> AlC <sub>2</sub>	0.5	CO <sub>2</sub> /N <sub>2</sub> CO <sub>2</sub> /CH <sub>4</sub>	70 29	93	25 °C, 4 bar, SG	Guan et al. (2021)

geneous distribution in the polymer matrix owing to the better compatibility of amino acids modified GO with Pebax matrix. The prepared MMMs containing arg@GO or his@GO showed much higher CO<sub>2</sub>/N<sub>2</sub> separation performance than GO/Pebax MMMs. The high CO<sub>2</sub> separation efficiency of MMMs containing arg@GO or his@GO resulted from the increased both the solubility selectivity and the diffusivity selectivity. The amine groups from amino acids enhanced the CO<sub>2</sub> solubility coefficient owing to the enhanced interaction between modified GO and CO<sub>2</sub> molecules via the reversible reaction and quadrupole moment interaction. The layered structure of GO increased the transport resistance for bigger N<sub>2</sub> molecules. The CO<sub>2</sub> permeability for arg@GO/Pebax and his@GO/Pebax MMMs was 169 Barrer and 149 Barrer, respectively. The determined CO<sub>2</sub>/N<sub>2</sub> selectivity was 70 and 50, respectively.

Voon et al. (2022) synthesized g-C<sub>3</sub>N<sub>4</sub> nanosheets and modified them with 4 types of functional groups. Fig. 9 shows the process of the preparation and modification of g-C<sub>3</sub>N<sub>4</sub> nanosheets. The modified g-C<sub>3</sub>N<sub>4</sub>/PIM-1 MMMs were fabricated for CO<sub>2</sub> separation. The unmodified g-C<sub>3</sub>N<sub>4</sub> could be homogeneously dispersed in the PIM-1 matrix when the filler loading was no more than 1 wt%, while the sulfonic group functionalized g-C<sub>3</sub>N<sub>4</sub> could be homogeneously dispersed in the PIM-1 matrix when the filler loading was no more than 10 wt%. This is because the sulfonic group functionalized g-C<sub>3</sub>N<sub>4</sub> possessed better compatibility

with the polymer matrix. Among the fabricated MMMs, PIM-1/g-C<sub>3</sub>N<sub>4</sub> (1 wt%) MMMs exhibited the highest CO<sub>2</sub> permeability and selectivity. The ultramicro pores (0.31 – 0.34 nm) from g-C<sub>3</sub>N<sub>4</sub> provided the additional pathways for smaller gas molecules such as CO<sub>2</sub> while inhibiting the transport of bigger gas molecules such as N<sub>2</sub> and CH<sub>4</sub>. In addition, the amine modification and sulfonation on g-C<sub>3</sub>N<sub>4</sub> nanosheets enhanced their affinity to CO<sub>2</sub> molecules, which increased the solubility coefficient of CO<sub>2</sub> molecules in MMMs.

Table 6 summarizes the separation efficiency of CO<sub>2</sub> molecules of MMMs containing 2D carbon-based materials. It can be found that GO and g-C<sub>3</sub>N<sub>4</sub> are usually modified and used as fillers in MMMs for gas separation. The filler content of 2D carbon-based materials is usually no more than 1 wt%, indicating the effectiveness of 2D carbon-based materials for the enhancement of CO<sub>2</sub> separation efficiency of MMMs. The post-synthetic modification strategy was often used to modify GO and g-C<sub>3</sub>N<sub>4</sub> with polar groups such as amine groups, and sulfonic groups.

### 3.3. MMMs containing Mxene

As an emerging material, 2D MXenes are promising fillers for the fabrication of MMMs for gas separation owing to their distinct properties such as the single atomic thickness, high mechanical stability,

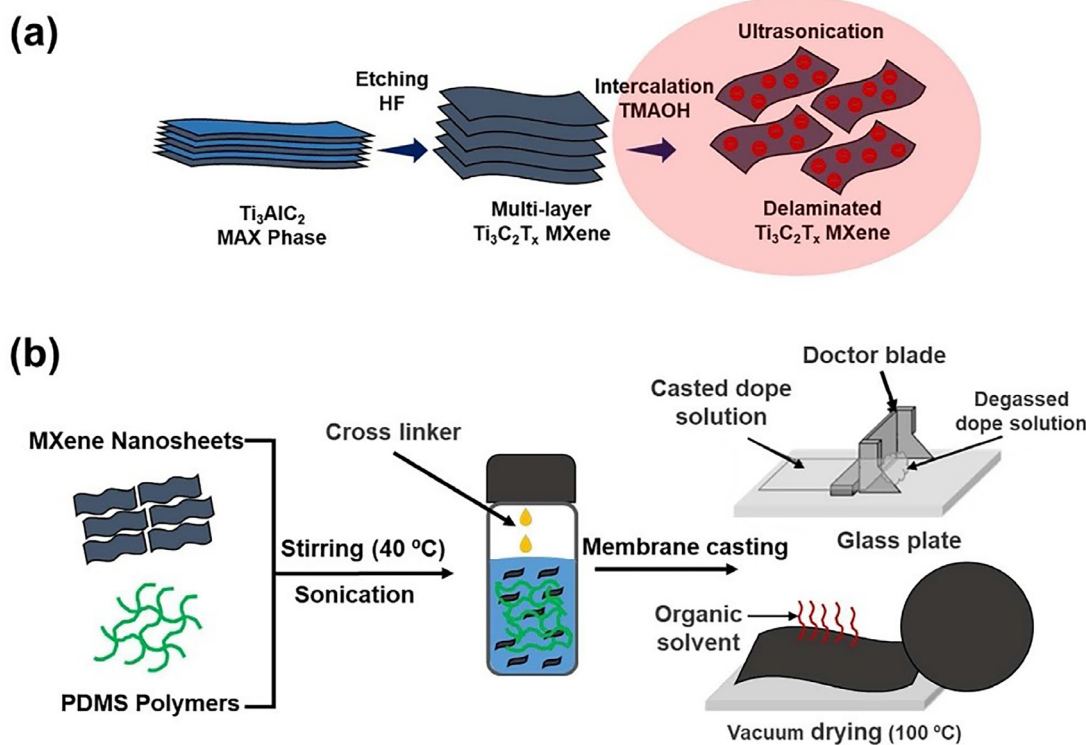


**Fig. 10.** (a) Synthesis of  $\text{Ti}_3\text{C}_2\text{T}_x$ -MXenes from MAX phase ( $\text{Ti}_3\text{AlC}_2$ ) and (b) Illustration of the fabrication of PDMS/ $\text{Ti}_3\text{C}_2\text{T}_x$ -MXene MMMs (Ahmad et al., 2023). Reprinted with permission from Elsevier. Copyright 2021.

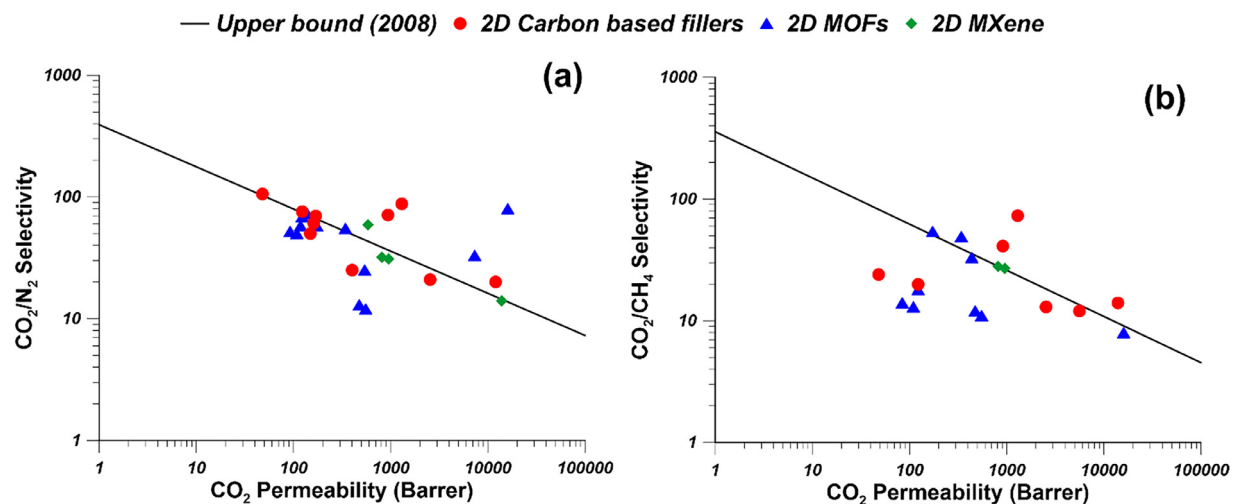


**Fig. 11.** The comparison of (a) CO<sub>2</sub>/N<sub>2</sub> separation performance and (b) CO<sub>2</sub>/CH<sub>4</sub> separation performance of MMMs containing 2D materials (data are from Tables 5–7).

and easy surface functionalization (Ahmad et al., 2023; Ramanavicius & Ramanavicius, 2020; Ahmed et al., 2021). MXenes are usually synthesized from 3D layered MAX phases. The synthesis methods of MXene nanosheets, the fabrication methods of MXene membranes, and their separation performance have been reviewed elsewhere (Ahmad et al., 2023; Ahmed et al., 2021). However, the review and discussion on the MMMs containing 2D MXene nanosheets is still lacking. As it is shown in Table 7, only a limited number of publications on MXene MMMs is available. To date, the most studied MXene in MMMs fabrication is  $\text{Ti}_3\text{C}_2\text{T}_x$ , even more than 150 various types of MAX phase have been reported (Mathis et al., 2021).

Ahmad et al. (2023) synthesized multi-layer MXene (ML-MXene) and single layer MXene (D-MXene) from the MAX phase  $\text{Ti}_3\text{AlC}_2$  by using the top-down synthesis method (Fig. 10a). Subsequently, the synthesized ML-MXene and D-MXene were incorporated into PDMS (Fig. 10b). The MMMs containing 1 wt% of D-MXene exhibited the highest CO<sub>2</sub> separation efficiency. The oxygen-functional groups of MXene show higher interaction with CO<sub>2</sub> molecules comparing with N<sub>2</sub> molecules, which facilitate the transport of CO<sub>2</sub> molecules.

Shi et al. (2021) prepared  $\text{Ti}_3\text{C}_2\text{T}_x$  MXene/Pebax 1657 and GO/Pebax 1657 MMMs and comparatively studied their effects on the membrane properties and gas permeation behavior.  $\text{Ti}_3\text{C}_2\text{T}_x$  MXene

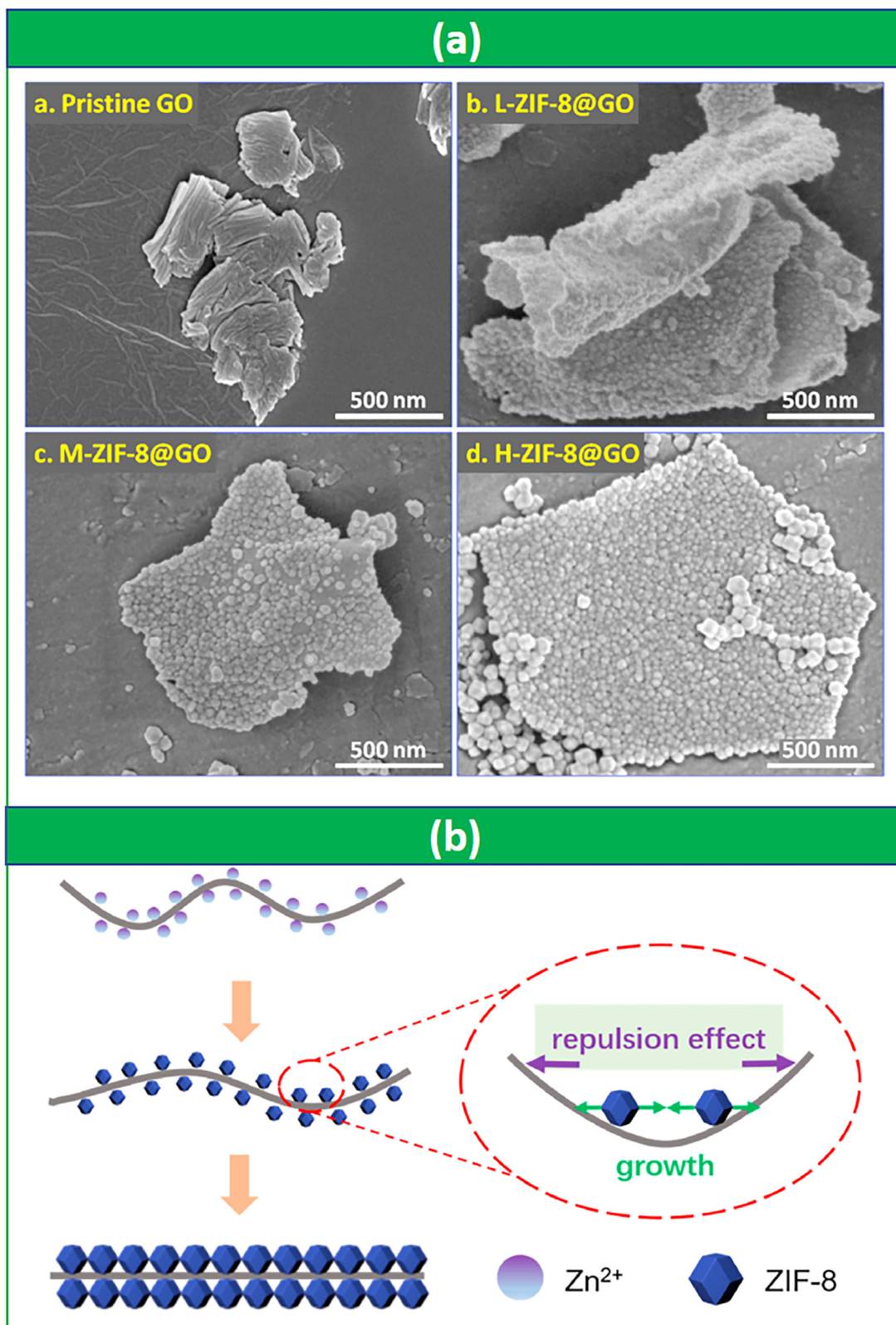


**Fig. 12.** (a) The pristine GO and the prepared ZIF-8@GO fillers with different ZIF-8/GO ratio (L, M, H-ZIF-8@GO); (b) The mechanism of GO stretching according to the ZIF-8 armor suit synthesis process (Yang et al., 2020). Reprinted with permission from Elsevier. Copyright 2020.

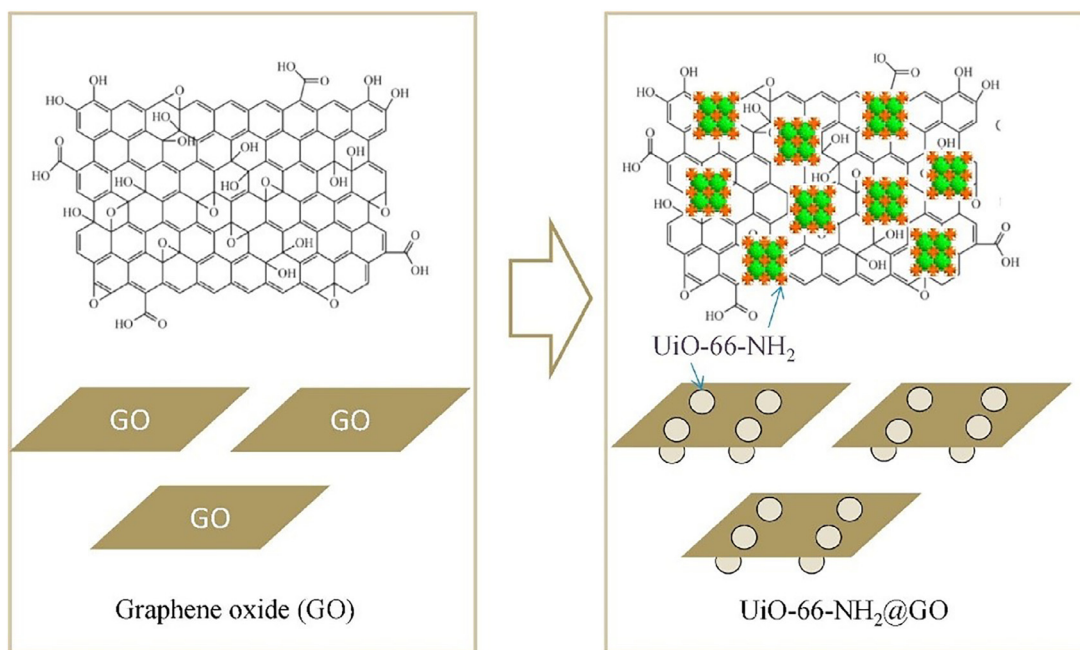


**Fig. 13.** The synthesis of UiO-66-NH<sub>2</sub>@GO by the formation of UiO-66-NH<sub>2</sub> particles on the GO nanosheets (Jia et al., 2019). Reprinted with permission from Elsevier. Copyright 2019.

could be incorporated into the Pebax 1657 matrix as high as 20 wt% while the maximum GO content was 5 wt%. This is because the abundant polar groups on MXene improved the interfacial interactions with the polymer matrix. MMMs containing 10 wt% of MXene exhibited CO<sub>2</sub> permeability of 584 Barrer and CO<sub>2</sub>/N<sub>2</sub> selectivity of 59 under humidified conditions. The high CO<sub>2</sub> separation efficiency under humidified conditions has resulted from the fast and selective CO<sub>2</sub> transport through the interlamellar channels of MXene in MMMs.

Fig. 11 shows the comparison between Robeson upper bound 2008 and the CO<sub>2</sub> separation efficiency of MMMs containing 2D MOFs, 2D carbon-based materials, and 2D MXene. All the MMMs containing 2D materials were located near or over the Robeson upper bound (2008). 2D materials possess a high potential to enhance the gas transport properties of MMMs.

#### 4. MMMs containing MOF based composite nanomaterials

The solution-diffusion and size-sieving mechanisms are mainly used to explain the gas transport behavior in MMMs (Yang et al., 2020; Hardian et al., 2024). To enhance the CO<sub>2</sub> separation performance of MMMs, the solubility and diffusivity of CO<sub>2</sub> molecules in MMMs should be enhanced to increase the CO<sub>2</sub> permeability. On the other hand, the size-sieving effect of MMMs should be enhanced to increase the selectivity further. MOFs possess high porosity, surface area, high affinity to CO<sub>2</sub> molecules, and good thermal stability (Kujawa et al., 2021). The incorporation of MOFs in MMMs could increase the solubility and diffusivity of CO<sub>2</sub> molecules, owing to their porous structure and high affinity to CO<sub>2</sub> molecules. Incorporating 2D materials such as GO in MMMs could create more tortuous diffusion pathways for bigger gas molecules (N<sub>2</sub> and CH<sub>4</sub>), slowing down the transport of bigger gas molecules and enhancing the CO<sub>2</sub> selectivity of membranes (Yang et al., 2020; Jia et al., 2019). Moreover, the MOF@GO composite fillers showed higher compatibility with the polymer matrix and can be homogeneously dispersed in the polymer matrix, owing to the nature of MOFs and the steric effect of GO. MOF@GO composite fillers combine the advantages of individual materials. Therefore, the incorporation of MOF@GO composite fillers could effectively enhance the CO<sub>2</sub> separation efficiency of MMMs.

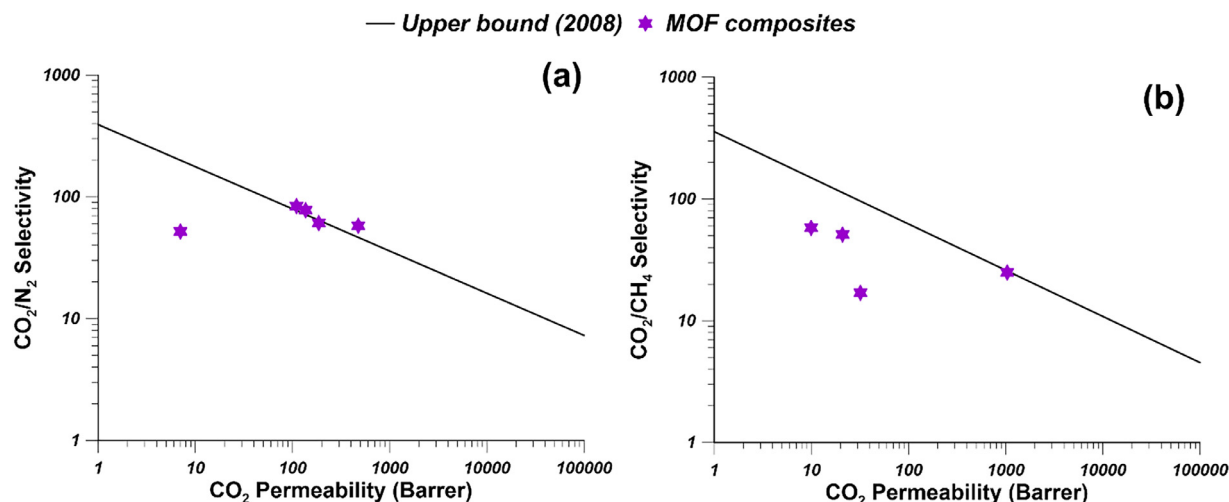
Yang et al. (2020) prepared ZIF-8@GO by growing ZIF-8 crystal on the GO surface, as shown in Fig. 12. Subsequently, the ZIF-8@GO/Pebax MMMs were fabricated. When the content of ZIF-8@GO was 20 wt%, MMMs demonstrated the highest CO<sub>2</sub> separation efficiency (CO<sub>2</sub> permeability of 136 Barrer and CO<sub>2</sub>/N<sub>2</sub> ideal selectivity of 78). This is because the additional CO<sub>2</sub> transporting channels were provided by porous ZIF-8. As a result, the CO<sub>2</sub> permeability increased. The CO<sub>2</sub>/N<sub>2</sub> selectivity was enhanced by abundant oxy-groups on the GO surface.

Jia et al. (2019) synthesized UiO-66-NH<sub>2</sub>@GO composite by growing UiO-66-NH<sub>2</sub> crystals on GO nanosheets, as shown in Fig. 13. Subsequently, UiO-66-NH<sub>2</sub>@GO/polyimide MMMs were fabricated for CO<sub>2</sub>/N<sub>2</sub> separation. The composite filler was homogeneously dispersed in a polyimide matrix owing to the high-aspect GO nanosheets. The CO<sub>2</sub> separation efficiency of MMMs was enhanced owing to the high porosity and the high CO<sub>2</sub> adsorption capacity of UiO-66-NH<sub>2</sub>@GO composite filler. Castarlenas et al. (Castarlenas et al., 2017) synthesized UiO-66-GO composite by growing UiO-66 on GO nanosheets via hydrothermal synthesis. Subsequently, UiO-66-GO/polyimide MMMs were prepared. UiO-66-GO composite showed good compatibility with polymer chains. The CO<sub>2</sub> separation efficiency of MMMs was enhanced owing to the barrier effect of GO and the porosity of UiO-66.

Besides the utilization of GO as carriers for the growth of MOFs, carbon nanotubes (CNTs) can be also used. CNTs could enhance the gas transport properties of MMMs since the CNT tunnels possess smooth internal walls. However, CNTs can easily aggregate, which makes it difficult to disperse them in the polymer matrix. The decoration of MOFs on CNTs can enhance the dispersion ability and compatibility in the polymer matrix (Lin et al., 2015). Lin et al. (2015) synthesized MIL@CNTs via the in situ growth of NH<sub>2</sub>-MIL-101(Al) on the external surface of CNTs. MIL@CNTs/polyimide MMMs were fabricated. CO<sub>2</sub> permeability and CO<sub>2</sub>/CH<sub>4</sub> selectivity of MMMs were increased comparing with the pristine membranes. The gas separation performance surpassed the Robeson upper bound. This is because the decoration of NH<sub>2</sub>-MIL-101(Al) on CNTs significantly increased the dispersion of CNTs in the polyimide matrix and the adsorption capacity of CO<sub>2</sub> and the CO<sub>2</sub>/CH<sub>4</sub> adsorption selectivity owing to the presence of amine groups. As a result, the membrane solubility coefficient of CO<sub>2</sub> was dramatically increased (Lin et al., 2015).

**Table 8**Separation efficiency of CO<sub>2</sub> molecules of MMMs containing MOF-based composite nanomaterials (SG - single gas, MG - mixed gas).

Polymers	MOF composites	Filler content [wt%]	Gas pairs	P <sub>CO<sub>2</sub></sub> [Barrer]	Selectivity	Testing conditions	Refs.
Matrimid®	UiO-66-NH <sub>2</sub> @GO	5	CO <sub>2</sub> /N <sub>2</sub>	7	52	25 °C, 3 bar, SG	Jia et al. (2019)
PEDM	ZIF-8@GO	6	CO <sub>2</sub> /N <sub>2</sub>	475	58	25 °C, 1 bar, SG	Chen et al. (2019)
Matrimid®	NiDOBDC/GO	20	CO <sub>2</sub> /CH <sub>4</sub>	10	58	25 °C, 1 bar, MG	Li et al. (2019)
Pebax	MWCNTs@ZIF-8	8	CO <sub>2</sub> /N <sub>2</sub>	186	61	35 °C, 5 bar, SG	Li et al. (2020)
Matrimid®	UiO-66-GO	24	CO <sub>2</sub> /CH <sub>4</sub>	21	51	35 °C, -, MG	Castarlenas et al. (2017)
6FDA-durene	NH <sub>2</sub> -MIL-101@CNT	10	CO <sub>2</sub> /CH <sub>4</sub>	1037	25	25 °C, 2 bar, SG	Lin et al. (2015)
PES	rGO-ZIF-8	2	CO <sub>2</sub> /CH <sub>4</sub>	8955 GPU	14	25 °C, 4 bar, SG	Jamil et al. (2019)
Pebax	ZIF-8@GO	20	CO <sub>2</sub> /N <sub>2</sub>	136	78	25 °C, 3 bar, SG	Yang et al. (2020)
Cellulose acetate	MWCNTs@ UiO-66-NH <sub>2</sub>	10	CO <sub>2</sub> /CH <sub>4</sub>	32	17	30 °C, -, MG	Tanvidkar et al. (2023)
Pebax 1657	ZIF-90@C <sub>3</sub> N <sub>4</sub>	8	CO <sub>2</sub> /N <sub>2</sub>	110	84	25 °C, 2 bar, SG	Guo et al. (2022)
Pebax 1657	ZIF-67@ZIF-L(Zn)	2	CO <sub>2</sub> /N <sub>2</sub>	73	103	25 °C, 4 bar, SG	Maleh & Raisi, 2023)
Pebax 1657	TA-ZIF-8/TCOH	0.184	CO <sub>2</sub> /N <sub>2</sub>	1178 GPU	63	25 °C, 1 bar, MG	Wang et al. (2024)
			CO <sub>2</sub> /CH <sub>4</sub>	1097 GPU	59		

**Fig. 14.** The comparison of (a) CO<sub>2</sub>/N<sub>2</sub> separation performance and (b) CO<sub>2</sub>/CH<sub>4</sub> separation performance of MMMs containing MOF composites (data are from Table 8).

According to the aforementioned discussion, the incorporation of MOF-based composite materials could enhance the CO<sub>2</sub> separation efficiency of MMMs owing to the synergistic effects of MOFs and carbon nanomaterials, e.g., GO and CNTs. Table 8 summarizes the CO<sub>2</sub> separation efficiency of MMMs containing MOF-based composite nanomaterials. For the synthesis of MOF composite nanomaterials, ZIF-8 (Yang et al., 2020; Chen et al., 2019; Li et al., 2020; Jamil et al., 2019), UiO-66 (Jia et al., 2019; Castarlenas et al., 2017), and MIL-101 (Lin et al., 2015) are the commonly used MOFs and GO (Yang et al., 2020; Jia et al., 2019; Castarlenas et al., 2017; Jamil et al., 2019), and CNT (Lin et al., 2015; Li et al., 2020) are the commonly used carbon nanomaterials. As it is shown in Fig. 14, the incorporation of MOF composites in MMMs could significantly improve the CO<sub>2</sub>/N<sub>2</sub> separation performance since most of the MMMs containing MOF composites surpassed the 2008 Robeson upper bound. However, the CO<sub>2</sub>/CH<sub>4</sub> separation performance was moderately improved since the MMMs containing MOF composites are close to but still below the 2008 Robeson upper bound.

## 5. Concluding remarks and future directions

This review provided a comprehensive summary on the modification of ZIFs, MOFs, and GO to prepare MMMs for CO<sub>2</sub> separation. After modification, the compatibility of fillers was significantly enhanced, resulting in homogeneous dispersion of fillers and enhanced mechanical stability and gas separation performance. Moreover, the modified

fillers could endow the MMMs with molecular sieving effects and facilitated transport mechanisms, which further increased the CO<sub>2</sub> permeability and selectivity simultaneously. In addition, this review provided an overview of the recent development of MMMs for CO<sub>2</sub> separation containing the emerging 2D MOFs, 2D MXene, and MOF composites. 2D materials could effectively regulate the gas transport pathways owing to their special layered structure and the size-sieving effect of the pores and space between layers. Moreover, the functional groups on the surface of 2D nanosheets provide active sites for further modification and improve the affinity to CO<sub>2</sub> molecules. As a result, MMMs containing modified ZIFs, MOFs and GO, 2D MOFs, 2D MXene, and MOF composites show high CO<sub>2</sub> separation performance since they are usually close to or above the Robeson upper bound.

This review shows that MMMs containing pristine and modified ZIFs, MOFs, and GO have been intensively studied for gas separation processes. However, in order to fully demonstrate the potential and capabilities of MMMs in CO<sub>2</sub> separation processes, the following directions still need more attention:

- As the emerging 2D materials, 2D MOFs and 2D MXene needs more attention in the fabrication of MMMs for gas separation. Even though various types of 2D MOFs have been synthesized and used in MMMs for gas separation, further modification of the existing 2D MOFs and the synthesis of new 2D MOFs are required. The most studied MXene in membrane fabrication is Ti<sub>3</sub>C<sub>2</sub>T<sub>x</sub>, and the synthesis and utilization of other types of MXene nanosheets in membrane preparation are highly needed.

2. The MOF@2D composites demonstrate positive effects on the improvement of gas separation performance of MMMs since they combined the advantages of 3D (MOFs) and 2D nanosheets. The synthesis and investigation of MOF@2D composites for the fabrication of MMMs is still limited in the literature. Therefore, further exploration of MOF@2D composites in MMMs for gas separation is highly needed.
3. In the industrial CO<sub>2</sub> separation processes, gas impurities and water vapor exist in CO<sub>2</sub>/N<sub>2</sub> and CO<sub>2</sub>/CH<sub>4</sub> mixtures. For example, flue gas mainly contains CO<sub>2</sub> and N<sub>2</sub>, along with impurities such as NO<sub>x</sub>, SO<sub>x</sub>, and volatile organic compounds. Besides the main components CO<sub>2</sub> and CH<sub>4</sub>, natural gas also contains impurities such as water vapor, He, and H<sub>2</sub>S. Most of research works from the literature focus on the study of CO<sub>2</sub> separation from a dual-component gas mixture rather than the multicomponent gas mixture. Therefore, the effect of gas impurities on the CO<sub>2</sub> separation performance and the structure change of MMMs should be investigated more in detail.

### Declaration of competing interest

The authors declare that they have no known competing financial interests or personal relationships that could have appeared to influence the work reported in this paper.

### CRediT authorship contribution statement

**Guoqiang Li:** Writing – review & editing, Writing – original draft, Visualization, Validation, Methodology, Conceptualization. **Joanna Kujawa:** Writing – original draft, Visualization, Validation, Conceptualization. **Katarzyna Knozowska:** Writing – original draft, Visualization. **Aivaras Kareiva:** Writing – review & editing, Formal analysis. **Eric Favre:** Writing – review & editing, Formal analysis. **Christophe Castel:** Writing – review & editing, Formal analysis. **Wojciech Kujawski:** Writing – review & editing, Validation, Supervision, Formal analysis, Conceptualization.

### References

- Abd, A.A., Othman, M.R., Naji, S.Z., Hashim, A.S., 2021. Methane enrichment in biogas mixture using pressure swing adsorption: process fundamental and design parameters. *Mater. Today Sustain.* 11–12, 100063.
- Ahmad, I., Alayande, A.B., Jee, H., Wang, Z., Park, Y.J., Im, K.S., Nam, S.Y., Bae, T.H., Yang, E., 2023. Recent progress of MXene-based membranes for high-performance and efficient gas separation. *Diam. Relat. Mater.* 135, 109883.
- Ahmad, I., Jee, H., Song, S.H., Kim, M.J., Eisa, T., Jang, J.K., Chae, K.J., Chuah, C.Y., Yang, E., 2023. Delaminated or Multi-layer Ti<sub>3</sub>C<sub>2</sub>T<sub>x</sub>-MXene-incorporated polydimethylsiloxane mixed matrix membrane for enhancing CO<sub>2</sub> /N<sub>2</sub> separation. *Mater. Today Sustain.* 23, 100410.
- Ahmad, M.Z., Navarro, M., Lhotka, M., Zornoza, B., Téllez, C., de Vos, W.M., Benes, N.E., Konnertz, N.M., Visser, T., Semino, R., Maurin, G., Fila, V., Coronas, J., 2018. Enhanced gas separation performance of 6FDA-DAM based mixed matrix membranes by incorporating MOF UiO-66 and its derivatives. *J. Membr. Sci.* 558, 64–77.
- Ahmed, Z., Rehman, F., Ali, U., Ali, A., Iqbal, M., Thebo, K.H., 2021. Recent advances in MXene-based separation membranes. *ChemBioEng Rev.* 8, 110–120.
- Aliyev, E., Warfsmann, J., Tokay, B., Shishatskiy, S., Lee, Y.J., Lillepaerg, J., Champness, N.R., Filiz, V., 2021. Gas transport properties of the metal–organic framework (MOF)-assisted polymer of intrinsic microporosity (PIM-1) thin-film composite membranes. *ACS Sustain. Chem. Eng.* 9, 684–694.
- Al-Rowaili, F.N., Khaled, M., Jamal, A., Zahid, U., 2023. Mixed matrix membranes for H<sub>2</sub>/CO<sub>2</sub> gas separation- a critical review. *Fuel* 333, 126285.
- Ashtiani, S., Khoshnamvand, M., Bouša, D., Šturala, J., Sofer, Z., Shaliutina-Kolešová, A., Gardenčík, D., Friess, K., 2021. Surface and interface engineering in CO<sub>2</sub>-philic based UiO-66-NH<sub>2</sub>-PEI mixed matrix membranes via covalently bridging PVP for effective hydrogen purification. *Int. J. Hydrol. Energy* 46, 5449–5458.
- Ban, Y., Li, Z., Li, Y., Peng, Y., Jin, H., Jiao, W., Guo, A., Wang, P., Yang, Q., Zhong, C., Yang, W., 2015. Confinement of ionic liquids in nanocages: tailoring the molecular sieving properties of ZIF-8 for membrane-based CO<sub>2</sub> capture. *Angew. Chem. Int. Ed.* 54, 15483–15487.
- Bano, S., Tariq, S.R., Anjum, T., Najam, M., Usman, M., Yasin, M., Shafi, H.Z., Khan, A.L., 2022. Development of highly permselective Mixed Matrix Membranes comprising of polyimide and Ln-MOF for CO<sub>2</sub> capture. *Chemosphere* 307, 136051.
- Biondo, L.D., Duarte, J., Zeni, M., Godinho, M., 2018. A Dual-mode model interpretation of CO<sub>2</sub>/CH<sub>4</sub> permeability in polysulfone membranes at low pressures. *An. Acad. Bras. Ciênc.* 90, 1855–1864.
- Casadei, R., Giacinti Baschetti, M., Yoo, M.J., Park, H.B., Giorgini, L., 2020. Pebax® 2533/graphene oxide nanocomposite membranes for carbon capture. *Membranes*. 10, 188.
- Castarlenas, S., Téllez, C., Coronas, J., 2017. Gas separation with mixed matrix membranes obtained from MOF UiO-66-graphite oxide hybrids. *J. Membr. Sci.* 526, 205–211.
- Chen, B., Wan, C., Kang, X., Chen, M., Zhang, C., Bai, Y., Dong, L., 2019. Enhanced CO<sub>2</sub> separation of mixed matrix membranes with ZIF-8@GO composites as fillers: Effect of reaction time of ZIF-8@GO. *Sep. Purif. Technol.* 223, 113–122.
- Chen, K., Ni, L., Guo, X., Xiao, C., Yang, Y., Zhou, Y., Zhu, Z., Qi, J., Li, J., 2023. Introducing pyrazole-based MOF to polymer of intrinsic microporosity for mixed matrix membranes with enhanced CO<sub>2</sub>/CH<sub>4</sub> separation performance. *J. Membr. Sci.* 688, 122110.
- Chen, K., Ni, L., Zhang, H., Xie, J., Yan, X., Chen, S., Qi, J., Wang, C., Sun, X., Li, J., 2021. Veiled metal organic frameworks nanofillers for mixed matrix membranes with enhanced CO<sub>2</sub>/CH<sub>4</sub> separation performance. *Sep. Purif. Technol.* 279, 119707.
- Chen, W., Zhang, Z., Hou, L., Yang, C., Shen, H., Yang, K., Wang, Z., 2020. Metal-organic framework MOF-801/PIM-1 mixed-matrix membranes for enhanced CO<sub>2</sub>/N<sub>2</sub> separation performance. *Sep. Purif. Technol.* 250, 117198.
- Chen, W., Zhang, Z., Yang, C., Liu, J., Shen, H., Yang, K., Wang, Z., 2021. PIM-based mixed-matrix membranes containing MOF-801/ionic liquid nanocomposites for enhanced CO<sub>2</sub> separation performance. *J. Membr. Sci.* 636, 119581.
- Chen, Z., Zhang, P., Wu, H., Sun, S., You, X., Yuan, B., Hou, J., Duan, C., Jiang, Z., 2022. Incorporating amino acids functionalized graphene oxide nanosheets into Pebax membranes for CO<sub>2</sub> separation. *Sep. Purif. Technol.* 288, 120682.
- Cheng, L., Song, Y., Chen, H., Liu, G., Liu, G., Jin, W., 2020. g-C<sub>3</sub>N<sub>4</sub> nanosheets with tunable affinity and sieving effect endowing polymeric membranes with enhanced CO<sub>2</sub> capture property. *Sep. Purif. Technol.* 250, 117200.
- Chuah, C.Y., Lee, J., Song, J., Bae, T.H., 2020. CO<sub>2</sub>/N<sub>2</sub> separation properties of polyimide-based mixed-matrix membranes comprising UiO-66 with various functionalities. *Membranes* 10, 154.
- Chuah, C.Y., Li, W., Samarasinghe, S.A.S.C., Sethunga, G.S.M.D.P., Bae, T.H., 2019. Enhancing the CO<sub>2</sub> separation performance of polymer membranes via the incorporation of amine-functionalized HKUST-1 nanocrystals. *Microporous Mesoporous Mater.* 290, 109680.
- Cui, J., Qi, D., Wang, X., 2018. Research on the techniques of ultrasound-assisted liquid-phase peeling, thermal oxidation peeling and acid-base chemical peeling for ultra-thin graphite carbon nitride nanosheets. *Ultrason. Sonochem.* 48, 181–187.
- Cui, Y., Cui, X., Yang, G., Yu, P., Wang, C., Kang, Z., Guo, H., Xia, D., 2024. High CO<sub>2</sub> adsorption of ultra-small Zr-MOF nanocrystals synthesized by modulation method boosts the CO<sub>2</sub>/CH<sub>4</sub> separation performance of mixed-matrix membranes. *J. Membr. Sci.* 689, 122174.
- Dai, Y., Niú, Z., Luo, W., Wang, Y., Mu, P., Li, J., 2023. A review on the recent advances in composite membranes for CO<sub>2</sub> capture processes. *Sep. Purif. Technol.* 307, 122752.
- Dai, Z., Deng, L., 2024. Membranes for CO<sub>2</sub> capture and separation: Progress in research and development for industrial applications. *Sep. Purif. Technol.* 335, 126022.
- Deng, J., Dai, Z., Deng, L., 2020. H<sub>2</sub>-selective Tröger's base polymer based mixed matrix membranes enhanced by 2D MOFs. *J. Membr. Sci.* 610, 118262.
- Ding, R., Li, Z., Dai, Y., Li, X., Ruan, X., Gao, J., Zheng, W., He, G., 2022. Boosting the CO<sub>2</sub>/N<sub>2</sub> selectivity of MMMs by vesicle shaped ZIF-8 with high amino content. *Sep. Purif. Technol.* 298, 121594.
- Ding, S.H., Oh, P.C., Mukhtar, H., Jamil, A., 2023. Nucleophilic substituted NH<sub>2</sub>-MIL-125 (Ti)/polyvinylidene fluoride hollow fiber mixed matrix membranes for CO<sub>2</sub>/CH<sub>4</sub> separation and CO<sub>2</sub> permeation prediction via theoretical models. *J. Membr. Sci.* 681, 121746.
- Du, X., Feng, S., Luo, J., Zhuang, Y., Song, W., Li, X., Wan, Y., 2023. Pebax mixed matrix membrane with bimetallic CeZr-MOFs to enhance CO<sub>2</sub> separation. *Sep. Purif. Technol.* 322, 124251.
- Duan, J., Li, Y., Pan, Y., Behera, N., Jin, W., 2019. Metal-organic framework nanosheets: An emerging family of multifunctional 2D materials. *Coord. Chem. Rev.* 395, 25–45.
- Esposito, E., Carta, M., Fuoco, A., Monteleone, M., Comesaña-Gándara, B., Gkniatou, E., Sicard, C., Wang, S., Serre, C., McKeown, N.B., Jansen, J.C., 2024. Single and mixed gas permeability studies on mixed matrix membranes composed of MIL-101(Cr) or MIL-177(Ti) and highly permeable polymers of intrinsic microporosity. *J. Membr. Sci.* 697, 122475.
- Fan, S.T., Tan, M., Liu, W.T., Li, B.J., Zhang, S., 2022. MOF-layer composite polyurethane membrane increasing both selectivity and permeability: Pushing commercial rubbery polymer membranes to be attractive for CO<sub>2</sub> separation. *Sep. Purif. Technol.* 297, 121452.
- Fan, Y., Li, C., Zhang, X., Yang, X., Su, X., Ye, H., Li, N., 2019. Tröger's base mixed matrix membranes for gas separation incorporating NH<sub>2</sub>-MIL-53(Al) nanocrystals. *J. Membr. Sci.* 573, 359–369.
- Feijani, E.A., Tavassoli, A., Mahdavi, H., Molavi, H., 2018. Effective gas separation through graphene oxide containing mixed matrix membranes. *J. Appl. Polym. Sci.* 135, 46271.
- Feng, S., Bu, M., Pang, J., Fan, W., Fan, L., Zhao, H., Yang, G., Guo, H., Kong, G., Sun, H., Kang, Z., Sun, D., 2020. Hydrothermal stable ZIF-67 nanosheets via morphology regulation strategy to construct mixed-matrix membrane for gas separation. *J. Membr. Sci.* 593, 117404.
- Feng, X., Qin, Z., Lai, Q., Zhang, Z., Shao, Z.W., Tang, W., Wu, W., Dai, Z., Liu, C., 2023. Mixed-matrix membranes based on novel hydroxamate metal-organic frameworks with two-dimensional layers for CO<sub>2</sub>/N<sub>2</sub> separation. *Sep. Purif. Technol.* 305, 122476.
- Ge, C., Sheng, M., Yuan, Y., Shi, F., Yang, Y., Zhao, S., Wang, J., Wang, Z., 2024. Pore-optimized MOF-808 made through a facile method using for fabrication of high-performance mixed matrix composite CO<sub>2</sub> capture membranes. *Carbon Capture Sci. Technol.* 10, 100156.
- George, G., Bhoria, N., AlHallaq, S., Abdala, A., Mittal, V., 2016. Polymer membranes for acid gas removal from natural gas. *Sep. Purif. Technol.* 158, 333–356.

- Gong, X.Y., Huang, Z.H., Zhang, H., Liu, W.L., Ma, X.H., Xu, Z.L., Tang, C.Y., 2020. Novel high-flux positively charged composite membrane incorporating titanium-based MOFs for heavy metal removal. *Chem. Eng. J.* 398, 125706.
- Gou, M., Zhu, W., Sun, Y., Guo, R., 2021. Introducing two-dimensional metal-organic frameworks with axial coordination anion into Pebax for CO<sub>2</sub>/CH<sub>4</sub> separation. *Sep. Purif. Technol.* 259, 118107.
- Guan, W., Yang, X., Dong, C., Yan, X., Zheng, W., Xi, Y., Ruan, X., Dai, Y., He, G., 2021. Prestructured MXene fillers with uniform channels to enhance CO<sub>2</sub> selective permeation in mixed matrix membranes. *J. Appl. Polym. Sci.* 138, 49895.
- Guo, A., Ban, Y., Yang, K., Yang, W., 2018. Metal-organic framework-based mixed matrix membranes: Synergistic effect of adsorption and diffusion for CO<sub>2</sub>/CH<sub>4</sub> separation. *J. Membr. Sci.* 562, 76–84.
- Guo, A., Ban, Y., Yang, K., Zhou, Y., Cao, N., Zhao, M., Yang, W., 2020. Molecular sieving mixed matrix membranes embodying nano-filters with extremely narrow pore-openings. *J. Membr. Sci.* 601, 117880.
- Guo, F., Li, D., Ding, R., Gao, J., Ruan, X., Jiang, X., He, G., Xiao, W., 2022. Constructing MOF-doped two-dimensional composite material ZIF-90@C<sub>3</sub>N<sub>4</sub> mixed matrix membranes for CO<sub>2</sub>/N<sub>2</sub> separation. *Sep. Purif. Technol.* 280, 119803.
- Habib, N., Durak, Ö., Uzun, A., Keskin, S., 2023. Incorporation of a pyrrolidinium-based ionic liquid/MIL-101(Cr) composite into Pebax sets a new benchmark for CO<sub>2</sub>/N<sub>2</sub> selectivity. *Sep. Purif. Technol.* 312, 123346.
- Habib, N., Shamair, Z., Tara, N., Nizami, A.S., Akhtar, F.H., Ahmad, N.M., Gilani, M.A., Bilad, M.R., Khan, A.L., 2020. Development of highly permeable and selective mixed matrix membranes based on Pebax®1657 and NOTT-300 for CO<sub>2</sub> capture. *Sep. Purif. Technol.* 234, 116101.
- Han, J., Bai, L., Jiang, H., Zeng, S., Yang, B., Bai, Y., Zhang, X., 2021. Task-specific ionic liquids tuning ZIF-67/PIM-1 mixed matrix membranes for efficient CO<sub>2</sub> separation. *Ind. Eng. Chem. Res.* 60, 593–603.
- Hardian, R., Jia, J., Diaz-Marquez, A., Naskar, S., Fan, D., Shekhah, O., Maurin, G., Edadaoui, M., Szekely, G., 2024. Design of mixed-matrix mof membranes with asymmetric filler density and intrinsic MOF/polymer compatibility for enhanced molecular sieving. *Adv. Mater.* 36, 2314206.
- Hasan, M.R., Zhao, H., Steunou, N., Serre, C., Malankowska, M., Téllez, C., Coronas, J., 2022. Optimization of MIL-178(Fe) and Pebax® 3533 loading in mixed matrix membranes for CO<sub>2</sub> capture. *Int. J. Greenh. Gas Control* 121, 103791.
- Husna, A., Hossain, I., Jeong, I., Kim, T.H., 2022. Mixed matrix membranes for efficient CO<sub>2</sub> separation using an engineered UiO-66 MOF in a pebax polymer. *Polymers* 14, 655.
- Imtiaz, A., Othman, M.H.D., Jilani, A., Khan, I.U., Kamaludin, R., Samuel, O., 2022. ZIF-filler incorporated mixed matrix membranes (MMMs) for efficient gas separation: A review. *J. Environ. Chem. Eng.* 10, 108541.
- Iqbal, Z., Shamair, Z., Usman, M., Gilani, M.A., Yasin, M., Saqib, S., Khan, A.L., 2022. One pot synthesis of UiO-66@IL composite for fabrication of CO<sub>2</sub> selective mixed matrix membranes. *Chemosphere* 303, 135122.
- Ishaq, S., Tamime, R., Bilad, M.R., Khan, A.L., 2019. Mixed matrix membranes comprising of polysulfone and microporous Bio-MOF-1: Preparation and gas separation properties. *Sep. Purif. Technol.* 210, 442–451.
- Jamil, N., Othman, N.H., Alias, N.H., Shahruddin, M.Z., Roslan, R.A., Lau, W.J., Ismail, A.F., 2019. Mixed matrix membranes incorporated with reduced graphene oxide (rGO) and zeolitic imidazole framework-8 (ZIF-8) nanofillers for gas separation. *J. Solid State Chem.* 270, 419–427.
- Jana, A., Modi, A., 2024. Recent progress on functional polymeric membranes for CO<sub>2</sub> separation from flue gases: A review. *Carbon Capture Sci. Technol.* 11, 100204.
- Jeong, S.K., Jeong, J.Y., Lim, S., Kim, W.S., Kwon, H.T., Kim, J., 2024. Mixed matrix membranes incorporating two-dimensional ZIF-8 nanosheets for enhanced CO<sub>2</sub>/N<sub>2</sub> separation. *Chem. Eng. J.* 481, 148294.
- Ji, L., Zhang, L., Zheng, X., Feng, L., He, Q., Wei, Y., Yan, S., 2021. Simultaneous CO<sub>2</sub> absorption, mineralisation and carbonate crystallisation promoted by amines in a single process. *J. CO<sub>2</sub> Util.* 51, 101653.
- Jia, M., Feng, Y., Qiu, J., Zhang, X.F., Yao, J., 2019. Amine-functionalized MOFs@GO as filler in mixed matrix membrane for selective CO<sub>2</sub> separation. *Sep. Purif. Technol.* 213, 63–69.
- Jia, M., Zhang, X.F., Zhou, Y., Mao, H., Zhao, Y., Yao, J., 2024. Amine-functionalized cellulose/UiO-66 composite membrane for facilitated CO<sub>2</sub> transport. *J. Membr. Sci.* 697, 122532.
- Jia, Y., Yang, J., Liu, P., Chen, K., Li, J., Pi, X., Han, C., Zhang, Y., 2024. Mixed matrix membranes containing oriented two-dimensional ZIF-L nanosheets for efficient H<sub>2</sub>/CO<sub>2</sub> separation. *Sep. Purif. Technol.* 338, 126589.
- Jiang, Y., Liu, C., Caro, J., Huang, A., 2019. A new UiO-66-NH<sub>2</sub> based mixed-matrix membranes with high CO<sub>2</sub>/CH<sub>4</sub> separation performance. *Microporous Mesoporous Mater.* 274, 203–211.
- Kamaludin, R., Xuefeng, M., Othman, M.H.D., Imtiaz, A., Hafiz Puteh, M., Kadir, S.H.S.A., 2023. ZIF-8-based dual layer hollow fiber mixed matrix membrane for natural gas purification. *Fuel* 354, 129377.
- Kamble, A.R., Patel, C.M., Murthy, Z.V.P., 2021. A review on the recent advances in mixed matrix membranes for gas separation processes. *Renew. Sustain. Energy Rev.* 145, 111062.
- Kang, M., Kim, T.H., Han, H.H., Min, H.J., Bae, Y.S., Kim, J.H., 2022. Submicron-thick, mixed-matrix membranes with metal-organic frameworks for CO<sub>2</sub> separation: MIL-140C vs. UIO-67. *J. Membr. Sci.* 659, 120788.
- Kujawa, J., Al-Gharabli, S., Muñoz, T.M., Knozowska, K., Li, G., Dumée, L.F., Kujawski, W., 2021. Crystalline porous frameworks as nano-enhancers for membrane liquid separation – Recent developments. *Coord. Chem. Rev.* 440, 213969.
- Lee, C.S., Moon, J., Park, J.T., Kim, J.H., 2023. Engineering CO<sub>2</sub>-philic pathway via grafting poly(ethylene glycol) on graphene oxide for mixed matrix membranes with high CO<sub>2</sub> permeance. *Chem. Eng. J.* 453, 139818.
- Li, B., Liu, J., He, X., Wang, R., Tao, W., Li, Z., 2023. Covalent “Bridge-crosslinking” strategy constructs facilitated transport mixed matrix membranes for highly-efficient CO<sub>2</sub> separation. *J. Membr. Sci.* 680, 121755.
- Li, E., Chen, Z., Duan, C., Yuan, B., Yan, S., Luo, X., Pan, F., Jiang, Z., 2022. Enhanced CO<sub>2</sub>-capture performance of polyimide-based mixed matrix membranes by incorporating ZnO@MOF nanocomposites. *Sep. Purif. Technol.* 289, 120714.
- Li, G., Kujawski, W., Tonkonogovas, A., Knozowska, K., Kujawa, J., Olewnik-Kruszkowska, E., Pedišius, N., Stankevičius, A., 2022. Evaluation of CO<sub>2</sub> separation performance with enhanced features of materials – Pebax® 2533 mixed matrix membranes containing ZIF-8-PEI@[P(3)HIm][Tf<sub>2</sub>N]. *Chem. Eng. Res. Des.* 181, 195–208.
- Li, G., Kujawski, W., Válek, R., Kotter, S., 2021. A review - The development of hollow fibre membranes for gas separation processes. *Int. J. Greenh. Gas Control* 104, 103195.
- Li, H., Tuo, L., Yang, K., Jeong, H.K., Dai, Y., He, G., Zhao, W., 2016. Simultaneous enhancement of mechanical properties and CO<sub>2</sub> selectivity of ZIF-8 mixed matrix membranes: Interfacial toughening effect of ionic liquid. *J. Membr. Sci.* 511, 130–142.
- Li, P., Wang, Z., Qiao, Z., Liu, Y., Cao, X., Li, W., Wang, J., Wang, S., 2015. Recent developments in membranes for efficient hydrogen purification. *J. Membr. Sci.* 495, 130–168.
- Li, W., Chuah, C.Y., Nie, L., Bae, T.H., 2019. Enhanced CO<sub>2</sub>/CH<sub>4</sub> selectivity and mechanical strength of mixed-matrix membrane incorporated with NiDOBDC/GO composite. *J. Ind. Eng. Chem.* 74, 118–125.
- Li, X., Yu, S., Li, K., Ma, C., Zhang, J., Li, H., Chang, X., Zhu, L., Xue, Q., 2020. Enhanced gas separation performance of Pebax mixed matrix membranes by incorporating ZIF-8 *in situ* inserted by multiwalled carbon nanotubes. *Sep. Purif. Technol.* 248, 117080.
- Liang, C., Huang, L., Lv, X., Wang, J., Li, L., Li, X., Wei, Z., 2023. Mixed matrix membranes based on ZIF-8 nanoparticles/Poly(4-styrene sulfonate) Fillers for enhanced CO<sub>2</sub> separation. *ACS Appl. Nano Mater.* 6, 2995–3002.
- Lin, R., Ge, L., Diao, H., Rudolph, V., Zhu, Z., 2016. Ionic liquids as the MOFs/polymer interfacial binder for efficient membrane separation. *ACS Appl. Mater. Interfaces* 8, 32041–32049.
- Lin, R., Ge, L., Liu, S., Rudolph, V., Zhu, Z., 2015. Mixed-matrix membranes with metal-organic framework-decorated CNT fillers for efficient CO<sub>2</sub> separation. *ACS Appl. Mater. Interfaces* 7, 14750–14757.
- Lin, Z., Yuan, Z., Wang, K., He, X., 2023. Synergistic tuning mixed matrix membranes by Ag<sup>+</sup>-doping in UiO-66-NH<sub>2</sub>/polymers of intrinsic microporosity for remarkable CO<sub>2</sub>/N<sub>2</sub> separation. *J. Membr. Sci.* 121775.
- Liu, B., Li, D., Yao, J., Sun, H., 2020. Improved CO<sub>2</sub> separation performance and interfacial affinity of mixed matrix membrane by incorporating UiO-66-PEI@[bmim][Tf<sub>2</sub>N] particles. *Sep. Purif. Technol.* 239, 116519.
- Liu, G., Cheng, L., Chen, G., Liang, F., Liu, G., Jin, W., 2020. Pebax-based membrane filled with two-dimensional mxene nanosheets for efficient CO<sub>2</sub> capture. *Chem. Asian J.* 15, 2364–2370.
- Liu, N., Cheng, J., Hou, W., Yang, C., Yang, X., Zhou, J., 2022. Bottom-up synthesis of two-dimensional composite via CuBDC-ns growth on multilayered MoS<sub>2</sub> to boost CO<sub>2</sub> permeability and selectivity in Pebax-based mixed matrix membranes. *Sep. Purif. Technol.* 282, 120007.
- Loiseau, T., Serre, C., Huguenard, C., Fink, G., Taullelle, F., Henry, M., Bataille, T., Férey, G., 2004. A rationale for the large breathing of the porous aluminum terephthalate (MIL-53) upon hydration. *Chem. Eur. J.* 10, 1373–1382.
- Lu, J., Zhang, X., Xu, L., Zhang, G., Zheng, J., Tong, Z., Shen, C., Meng, Q., 2021. Preparation of amino-functionalized UiO-66/PIMs mixed matrix membranes with [bmim][Tf<sub>2</sub>N] as regulator for enhanced gas separation. *Membranes* 11, 35.
- Luo, W., Niu, Z., Mu, P., Li, J., 2022. MXene/poly(ethylene glycol) mixed matrix membranes with excellent permeance for highly efficient separation of CO<sub>2</sub>/N<sub>2</sub> and CO<sub>2</sub>/CH<sub>4</sub>. *Colloids Surf. A Physicochem. Eng. Asp.* 640, 128481.
- Luque-Alled, J.M., Ameen, A.W., Alberto, M., Tamaddor, M., Foster, A.B., Budd, P.M., Vijayaraghavan, A., Gorgojo, P., 2021. Gas separation performance of MMMs containing (PIM-1)-functionalized GO derivatives. *J. Membr. Sci.* 623, 118902.
- Ma, Y., He, X., Tang, S., Xu, S., Qian, Y., Zeng, L., Tang, K., 2022. Enhanced 2-D MOFs nanosheets/PIM-PMDA-OH mixed matrix membrane for efficient CO<sub>2</sub> separation. *J. Environ. Chem. Eng.* 10, 107274.
- Mahajan, S., Lahtinen, M., 2022. Recent progress in metal-organic frameworks (MOFs) for CO<sub>2</sub> capture at different pressures. *J. Environ. Chem. Eng.* 10, 108930.
- Majumdar, S., Tokay, B., Martin-Gil, V., Campbell, J., Castro-Muñoz, R., Ahmad, M.Z., Fila, V., 2020. Mg-MOF-74/Polyvinyl acetate (PVAc) mixed matrix membranes for CO<sub>2</sub> separation. *Sep. Purif. Technol.* 238, 116411.
- Maleh, M.S., Raisi, A., 2023. Heteroepitaxial growth of ZIF-67 nanoparticles on the ZIF-L(Zn) nanosheets for fabrication of Pebax mixed matrix membranes with highly efficient CO<sub>2</sub> separation. *Chemosphere* 344, 140249.
- Maleh, M.S., Raisi, A., 2023. Experimental and modeling study on interfacial morphology of ZIF-67/Pebax-2533 mixed matrix membranes for CO<sub>2</sub> separation applications. *Surf. Interfaces* 38, 102846.
- Mathis, T.S., Maleski, K., Goad, A., Sarycheva, A., Anayee, M., Foucher, A.C., Hantanasisirakul, K., Shuck, C.E., Stach, E.A., Gogotsi, Y., 2021. Modified MAX phase synthesis for environmentally stable and highly conductive Ti<sub>3</sub>C<sub>2</sub> MXene. *ACS Nano* 15, 6420–6429.
- Mehdinia Lichlai, M., Pazani, F., Aroujalian, A., Rodriguez, D., 2022. Two-step surface functionalization/alignment strategy to improve CO<sub>2</sub>/N<sub>2</sub> separation from mixed matrix membranes based on PEBAK and graphene oxide. *Process Saf. Environ. Prot.* 163, 36–47.
- Min, H.J., Kang, M., Bae, Y.S., Blom, R., Grande, C.A., Kim, J.H., 2023. Thin-film composite mixed-matrix membrane with irregular micron-sized UTSA-16 for outstanding gas separation performance. *J. Membr. Sci.* 669, 121295.

- Mohammed, S.A., Nasir, A.M., Aziz, F., Kumar, G., Sallehudin, W., Jaafar, J., Lau, W.J., Yusof, N., Salleh, W.N.W., Ismail, A.F., 2019. CO<sub>2</sub>/N<sub>2</sub> selectivity enhancement of PE-BAX MH 1657/Aminated partially reduced graphene oxide mixed matrix composite membrane. *Sep. Purif. Technol.* 223, 142–153.
- Mohsenpour, S., Ameen, A.W., Leaper, S., Skuse, C., Almansour, F., Budd, P.M., Gorjoo, P., 2022. PIM-1 membranes containing POSS - graphene oxide for CO<sub>2</sub> separation. *Sep. Purif. Technol.* 298, 121447.
- Mubashir, M., Yin fong, Y., Leng, C.T., Keong, L.K., Jusoh, N., 2020. Study on the effect of process parameters on CO<sub>2</sub>/CH<sub>4</sub> binary gas separation performance over NH<sub>2</sub>-MIL-53(Al)/cellulose acetate hollow fiber mixed matrix membrane. *Polym. Test.* 81, 106223.
- Nobakht, D., Abedini, R., 2023. A new ternary Pebax®1657/maltitol/ZIF-8 mixed matrix membrane for efficient CO<sub>2</sub> separation. *Process Saf. Environ. Prot.* 170, 709–719.
- Ozcan, A., Fan, D., Datta, S.J., Diaz-Marquez, A., Semino, R., Cheng, Y., Joarder, B., Edaoudi, M., Maurin, G., 2024. Tuning MOF/polymer interfacial pore geometry in mixed matrix membrane for upgrading CO<sub>2</sub> separation performance. *Sci. Adv.* 10, eadk5846.
- Pang, S., Li, Y., Chen, X., Huang, A., 2023. C-axis oriented ZIF-95 sheets intermixed with polyimide matrix with enhanced gas separation performance. *J. Membr. Sci.* 679, 121696.
- Pasichnyk, M., Stanovsky, P., Polezhaev, P., Zach, B., Šyc, M., Bobák, M., Jansen, J.C., Přibyl, M., Bara, J.E., Friess, K., Havlicek, J., Gin, D.L., Noble, R.D., Izák, P., 2023. Membrane technology for challenging separations: Removal of CO<sub>2</sub>, SO<sub>2</sub> and NOx from flue and waste gases. *Sep. Purif. Technol.* 323, 124436.
- Pazani, F., Aroujalian, A., 2020. Enhanced CO<sub>2</sub>-selective behavior of pebax-1657: A comparative study between the influence of graphene-based fillers. *Polym. Test.* 81, 106264.
- Pu, Y., Yang, Z., Wee, V., Wu, Z., Jiang, Z., Zhao, D., 2022. Amino-functionalized NUS-8 nanosheets as fillers in PIM-1 mixed matrix membranes for CO<sub>2</sub> separations. *J. Membr. Sci.* 641, 119912.
- Qin, Z., Ma, Y., Du, W., Wei, J., Song, J., Fan, X., Yao, L., Yang, L., Zhuang, Y., Jiang, W., Dai, Z., 2024. Mixed matrix membranes (MMMs) with amine-functionalized ZIF-L for enhanced CO<sub>2</sub> separation performance. *Sep. Purif. Technol.* 126831.
- Ramanavicius, S., Ramanavicius, A., 2020. Progress and insights in the application of MXenes as new 2D nano-materials suitable for biosensors and biofuel cell design. *Int. J. Mol. Sci.* 21, 9224.
- Rego, R.M., Kurkuri, M.D., Kigga, M., 2022. A comprehensive review on water remediation using UiO-66 MOFs and their derivatives. *Chemosphere* 302, 134845.
- Robeson, L.M., 2008. The upper bound revisited. *J. Membr. Sci.* 320, 390–400.
- Sasikumar, B., Arthanareeswaran, G., 2022. Interfacial design of polysulfone/Cu-BTC membrane using [Bmim][TF2N] and [Dmim][Cl] RTILs for CO<sub>2</sub> separation: Performance assessment for single and mixed gas separation. *Sep. Purif. Technol.* 295, 121315.
- Sasikumar, B., Arthanareeswaran, G., 2022. Construction of selective gas permeation channels in polymeric membranes using nanocage tuned ionic liquid/MIL-53 (Al) filler nanoparticles for effective CO<sub>2</sub> separation. *J. Nat. Gas. Sci. Eng.* 106, 104728.
- Schneemann, A., Bon, V., Schwedler, I., Senkovska, I., Kaskel, S., Fischer, R.A., 2014. Flexible metal-organic frameworks. *Chem. Soc. Rev.* 43, 6062–6096.
- Shamsabadi, A.A., Isfahani, A.P., Salestan, S.K., Rahimpour, A., Ghalei, B., Sivaniah, E., Soroush, M., 2020. Pushing rubbery polymer membranes to be economic for CO<sub>2</sub> separation: embedment with Ti<sub>3</sub>C<sub>2</sub>T<sub>x</sub> MXene nanosheets. *ACS Appl. Mater. Interfaces* 12, 3984–3992.
- Shi, F., Sun, J., Wang, J., Liu, M., Yan, Z., Zhu, B., Li, Y., Cao, X., 2021. MXene versus graphene oxide: Investigation on the effects of 2D nanosheets in mixed matrix membranes for CO<sub>2</sub> separation. *J. Membr. Sci.* 620, 118850.
- Song, C., Li, R., Fan, Z., Liu, Q., Zhang, B., Kitamura, Y., 2020. CO<sub>2</sub>/N<sub>2</sub> separation performance of Pebax/MIL-101 and Pebax /NH<sub>2</sub>-MIL-101 mixed matrix membranes and intensification via sub-ambient operation. *Sep. Purif. Technol.* 238, 116500.
- Suhaimi, N.H., Yeong, Y.F., Jusoh, N., Chew, T.L., Bustam, M.A., Suleiman, S., 2020. Separation of CO<sub>2</sub> from CH<sub>4</sub> using mixed matrix membranes incorporated with amine functionalized MIL-125 (Ti) nanofiller. *Chem. Eng. Res. Des.* 159, 236–247.
- Sun, Y., Geng, C., Zhang, Z., Qiao, Z., Zhong, C., 2022. Two-dimensional basic cobalt carbonate supported ZIF-67 composites towards mixed matrix membranes for efficient CO<sub>2</sub>/N<sub>2</sub> separation. *J. Membr. Sci.* 661, 120928.
- Tanvidkar, P., Nayak, B., Kuncharam, B.V.R., 2023. Study of dual filler mixed matrix membranes with acid-functionalized MWCNTs and metal-organic framework (UiO-66-NH<sub>2</sub>) in cellulose acetate for CO<sub>2</sub> separation. *J. Polym. Environ.* 31, 3404–3417.
- Thür, R., Van Velthoven, N., Slootmaekers, S., Didden, J., Verbeke, R., Smolders, S., Dickmann, M., Egger, W., De Vos, D., Vankelecom, I.F.J., 2019. Bipyridine-based UiO-67 as novel filler in mixed-matrix membranes for CO<sub>2</sub>-selective gas separation. *J. Membr. Sci.* 576, 78–87.
- van Essen, M., van den Akker, L., Thür, R., Houben, M., Vankelecom, I.F.J., Borneman, Z., Nijmeijer, K., 2021. The influence of pore aperture, volume and functionality of isoreticular gemelinite zeolitic imidazolate frameworks on the mixed gas CO<sub>2</sub>/N<sub>2</sub> and CO<sub>2</sub>/CH<sub>4</sub> separation performance in mixed matrix membranes. *Sep. Purif. Technol.* 260, 118103.
- Voon, B.K., Shen Lau, H., Liang, C.Z., Yong, W.F., 2022. Functionalized two-dimensional g-C<sub>3</sub>N<sub>4</sub> nanosheets in PIM-1 mixed matrix membranes for gas separation. *Sep. Purif. Technol.* 296, 121354.
- Wang, C., Wu, J., Cheng, P., Xu, L., Zhang, S., 2023. Nanocomposite polymer blend membrane molecularly re-engineered with 2D metal-organic framework nanosheets for efficient membrane CO<sub>2</sub> capture. *J. Membr. Sci.* 685, 121950.
- Wang, D., Ying, Y., Zheng, Y., Pu, Y., Yang, Z., Zhao, D., 2022. Induced polymer crystallinity in mixed matrix membranes by metal-organic framework nanosheets for gas separation. *J. Membr. Sci. Letters* 2, 100017.
- Wang, F., Wang, Z., Yu, J., Han, S., Li, X., Wang, Y., 2024. Mixed matrix membranes with intrinsic microporous/UiO-66 post-synthesis modifications with no defects for efficient CO<sub>2</sub>/N<sub>2</sub> separation. *Sep. Purif. Technol.* 333, 125892.
- Wang, J., Li, L., Zhang, J., Li, X., 2024. Boosting CO<sub>2</sub> transport in mixed matrix membranes by chitosan-MOF networks. *J. Membr. Sci.* 697, 122569.
- Wang, Y., Dai, Y., Ruan, X., Zheng, W., Yan, X., Li, X., He, G., 2021. ZIF-8 hollow nanotubes based mixed matrix membranes with high-speed gas transmission channel to promote CO<sub>2</sub>/N<sub>2</sub> separation. *J. Membr. Sci.* 630, 119323.
- Wang, Y., Ren, Y., Wu, H., Wu, X., Yang, H., Yang, L., Wang, X., Wu, Y., Liu, Y., Jiang, Z., 2020. Amino-functionalized ZIF-7 embedded polymers of intrinsic micro-porosity membrane with enhanced selectivity for biogas upgrading. *J. Membr. Sci.* 602, 117970.
- Wang, Y., Yang, G., Guo, H., Meng, X., Kong, G., Kang, Z., Guillet-Nicolas, R., Mintova, S., 2022. Preparation of HKUST-1/PEI mixed-matrix membranes: Adsorption-diffusion coupling control of small gas molecules. *J. Membr. Sci.* 643, 120070.
- Wang, Y., Zhong, S., Li, S., Dai, Y., Su, W., Li, J., 2024. Pod-like TA-ZIF-8/TCOH composite filler for the preparation of mixed matrix membrane for efficient CO<sub>2</sub> separation. *J. Membr. Sci.* 697, 122524.
- Wang, Z., Yuan, J., Li, R., Zhu, H., Duan, J., Guo, Y., Liu, G., Jin, W., 2021. ZIF-301 MOF/6FDA-DAM polyimide mixed-matrix membranes for CO<sub>2</sub>/CH<sub>4</sub> separation. *Sep. Purif. Technol.* 264, 118431.
- Weng, Q., Wang, X., Wang, X., Bando, Y., Golberg, D., 2016. Functionalized hexagonal boron nitride nanomaterials: emerging properties and applications. *Chem. Soc. Rev.* 45, 3989–4012.
- Wu, C., Guo, H., Liu, X., Zhang, B., 2022. Mixed matrix membrane comprising glycine grafted CuBTC for enhanced CO<sub>2</sub> separation performances with excellent stability under humid atmosphere. *Sep. Purif. Technol.* 295, 121287.
- Wu, C.Y., Chang, B.K., 2024. Effect of ZIF-78 metal-organic framework crystal morphology and defect in resulting polysulfone mixed matrix membranes. *J. Taiwan. Inst. Chem. Eng.* 157, 105418.
- Xin, Q., Cao, X., Huang, D., Li, S., Zhang, X., Xuan, G., Wei, M., Zhang, L., Ding, X., Zhang, Y., 2022. Smart light-responsive hierarchical metal organic frameworks constructed mixed matrix membranes for efficient gas separation. *Green Chem. Eng.* 3, 71–82.
- Xin, Q., Li, S., Ma, F., Guo, J., Wang, S., Xuan, G., Ding, X., Zhang, L., Zhang, Y., 2022. Pebax-based membrane filled with photo-responsive Azo@NH<sub>2</sub>-MIL-53 nanoparticles for efficient SO<sub>2</sub>/N<sub>2</sub> separation. *Sep. Purif. Technol.* 296, 121363.
- Xin, Q., Ma, F., Zhang, L., Wang, S., Li, Y., Ye, H., Ding, X., Lin, L., Zhang, Y., Cao, X., 2019. Interface engineering of mixed matrix membrane via CO<sub>2</sub>-philic polymer brush functionalized graphene oxide nanosheets for efficient gas separation. *J. Membr. Sci.* 586, 23–33.
- Xu, J., Wu, H., Wang, Z., Qiao, Z., Zhao, S., Wang, J., 2018. Recent advances on the membrane processes for CO<sub>2</sub> separation. *Chin. J. Chem. Eng.* 26, 2280–2291.
- Xu, R., Wang, Z., Wang, M., Qiao, Z., Wang, J., 2019. High nanoparticles loadings mixed matrix membranes via chemical bridging-crosslinking for CO<sub>2</sub> separation. *J. Membr. Sci.* 573, 455–464.
- Yahia, M., Lozano, L.A., Zamora, J.M., Téllez, C., Coronas, J., 2024. Microwave-assisted synthesis of metal-organic frameworks UiO-66 and MOF-808 for enhanced CO<sub>2</sub>/CH<sub>4</sub> separation in PIM-1 mixed matrix membranes. *Sep. Purif. Technol.* 330, 125558.
- Yang, E., Goh, K., Chuah, C.Y., Wang, R., Bae, T.H., 2020. Asymmetric mixed-matrix membranes incorporated with nitrogen-doped graphene nanosheets for highly selective gas separation. *J. Membr. Sci.* 615, 118293.
- Yang, K., Dai, Y., Ruan, X., Zheng, W., Yang, X., Ding, R., He, G., 2020. Stretched ZIF-8@GO flake-like fillers via pre-Zn(II)-doping strategy to enhance CO<sub>2</sub> permeation in mixed matrix membranes. *J. Membr. Sci.* 601, 117934.
- Yang, X., Zheng, W., Xi, Y., Guan, W., Yan, X., Ruan, X., Ma, C., Dai, Y., He, G., 2021. Constructing low-resistance and high-selectivity transport multi-channels in mixed matrix membranes for efficient CO<sub>2</sub> separation. *J. Membr. Sci.* 624, 119046.
- Yang, Z., Ying, Y., Pu, Y., Wang, D., Yang, H., Zhao, D., 2022. Poly(ionic liquid)-functionalized UiO-66(OH)<sub>2</sub>: improved interfacial compatibility and separation ability in mixed matrix membranes for CO<sub>2</sub> separation. *Ind. Eng. Chem. Res.* 61, 7626–7633.
- Yao, B.J., Ding, L.G., Li, F., Li, J.T., Fu, Q.J., Ban, Y., Guo, A., Dong, Y.B., 2017. Chemically cross-linked MOF membrane generated from imidazolium-based ionic liquid-decorated UiO-66 type NMOF and its application toward CO<sub>2</sub> separation and conversion. *ACS Appl. Mater. Interfaces* 9, 38919–38930.
- Ye, C., Wu, X., Wu, H., Yang, L., Ren, Y., Wu, Y., Liu, Y., Guo, Z., Zhao, R., Jiang, Z., 2020. Incorporating nano-sized ZIF-67 to enhance selectivity of polymers of intrinsic microporosity membranes for biogas upgrading. *Chem. Eng. Sci.* 216, 115497.
- Yin, H., Alkaş, A., Zhang, Y., Zhang, Y., Telfer, S.G., 2020. Mixed matrix membranes (MMMs) using an emerging metal-organic framework (MUF-15) for CO<sub>2</sub> separation. *J. Membr. Sci.* 609, 118245.
- Yousef, A.M., El-Maghly, W.M., Eldrainy, Y.A., Attia, A., 2018. New approach for biogas purification using cryogenic separation and distillation process for CO<sub>2</sub> capture. *Energy* 156, 328–351.
- Yu, H.J., Chiou, D.S., Hsu, C.H., Tsai, H.Y., Kan, M.Y., Lee, J.S., Kang, D.Y., 2022. Engineering CAU-10-H in the preparation of mixed matrix membranes for gas separation. *J. Membr. Sci.* 663, 121024.
- Zhang, J., Xin, Q., Li, X., Yun, M., Xu, R., Wang, S., Li, Y., Lin, L., Ding, X., Ye, H., Zhang, Y., 2019. Mixed matrix membranes comprising aminosilane-functionalized graphene oxide for enhanced CO<sub>2</sub> separation. *J. Membr. Sci.* 570–571, 343–354.
- Zhang, M., Semiat, R., He, X., 2022. Recent advances in Poly(ionic liquids) membranes for CO<sub>2</sub> separation. *Sep. Purif. Technol.* 299, 121784.

- Zhang, Q., Zhou, M., Liu, X., Zhang, B., 2021. Pebax/two-dimensional MFI nanosheets mixed-matrix membranes for enhanced CO<sub>2</sub> separation. *J. Membr. Sci.* 636, 119612.
- Zhang, X., Zhang, T., Wang, Y., Li, J., Liu, C., Li, N., Liao, J., 2018. Mixed-matrix membranes based on Zn/Ni-ZIF-8-PEBA for high performance CO<sub>2</sub> separation. *J. Membr. Sci.* 560, 38–46.
- Zhao, Q., Lian, S., Li, R., Yang, Y., Zang, G., Song, C., 2023. Fabricating leaf-like hierarchical ZIF-67 as intra-mixed matrix membrane microarchitecture for efficient intensification of CO<sub>2</sub> separation. *Sep. Purif. Technol.* 305, 122460.
- Zhao, Q., Sun, Y., Zhang, J., Fan, F., Li, T., He, G., Ma, C., 2024. Mixed matrix membranes incorporating amino-functionalized ZIF-8-NH<sub>2</sub> in a carboxylic polyimide for molecularly selective gas separation. *J. Membr. Sci.* 693, 122326.
- Zhou, Y., Jia, M., Zhang, X., Yao, J., 2020. Etched ZIF-8 as a filler in mixed-matrix membranes for enhanced CO<sub>2</sub>/N<sub>2</sub> separation. *Chem. Eur. J.* 26, 7918–7922.
- Zhou, Z., Cao, X., Lv, D., Cheng, F., 2024. Hydrophobic metal-organic framework UiO-66-(CF<sub>3</sub>)<sub>2</sub>/PIM-1 mixed-matrix membranes for stable CO<sub>2</sub>/N<sub>2</sub> separation under high humidity. *Sep. Purif. Technol.* 339, 126666.
- Zhu, C., Peng, Y., Yang, W., 2021. Modification strategies for metal-organic frameworks targeting at membrane-based gas separations. *Green Chem. Eng.* 2, 17–26.
- Zhu, H., Jie, X., Wang, L., Kang, G., Liu, D., Cao, Y., 2018. Enhanced gas separation performance of mixed matrix hollow fiber membranes containing post-functionalized S-MIL-53. *J. Energy Chem.* 27, 781–790.
- Zhu, W., Wang, L., Cao, H., Guo, R., Wang, C., 2023. Introducing defect-engineering 2D layered MOF nanosheets into Pebax matrix for CO<sub>2</sub>/CH<sub>4</sub> separation. *J. Membr. Sci.* 669, 121305.
- Zou, D., Liu, D., 2019. Understanding the modifications and applications of highly stable porous frameworks via UiO-66. *Mater. Today Chem.* 12, 139–165.